

Thin films: new physics and applications ?

Oberseminar 2007

Hao Tjeng

**Lehrstuhl für Angewandte Physik
II. Physikalisches Institut, Universität zu Köln**

Can we use thin films to create new materials, new properties and new devices ?

Yes, but one needs to understand the 'physics', i.e. need to understand what happens to the electronic structure !

- Modification of material properties due to proximity of substrate:
 - strain
 - screening
 - charge donation
- New material compositions:
non-existent in bulk, but stabilized in film
- New sample preparation routes:
MBE combined with distillation and
control of stoichiometry during growth by resistivity measurements

Can we use thin films to create new materials, new properties and new devices ?

Yes, but one needs to understand the ‘physics’, i.e. need to understand what happens to the electronic structure !

- Modification of material properties due to proximity of substrate:

- strain

- screening

- charge donation

- New material compositions:

- non-existent in bulk, but stabilized in film

- New sample preparation routes:

- MBE combined with distillation and

- control of stoichiometry during growth by resistivity measurements

Nature 394, 453 (1998).

Doubling the critical temperature of $\text{La}_{1.9}\text{Sr}_{0.1}\text{CuO}_4$ using epitaxial strain

J.-P. Locquet*, J. Perret†, J. Fompeyrine‡, E. Mächler*, J. W. Seo† & G. Van Tendeloo§

* IBM Research Division, Zurich Research Laboratory, CH-8803 Rüschlikon, Switzerland

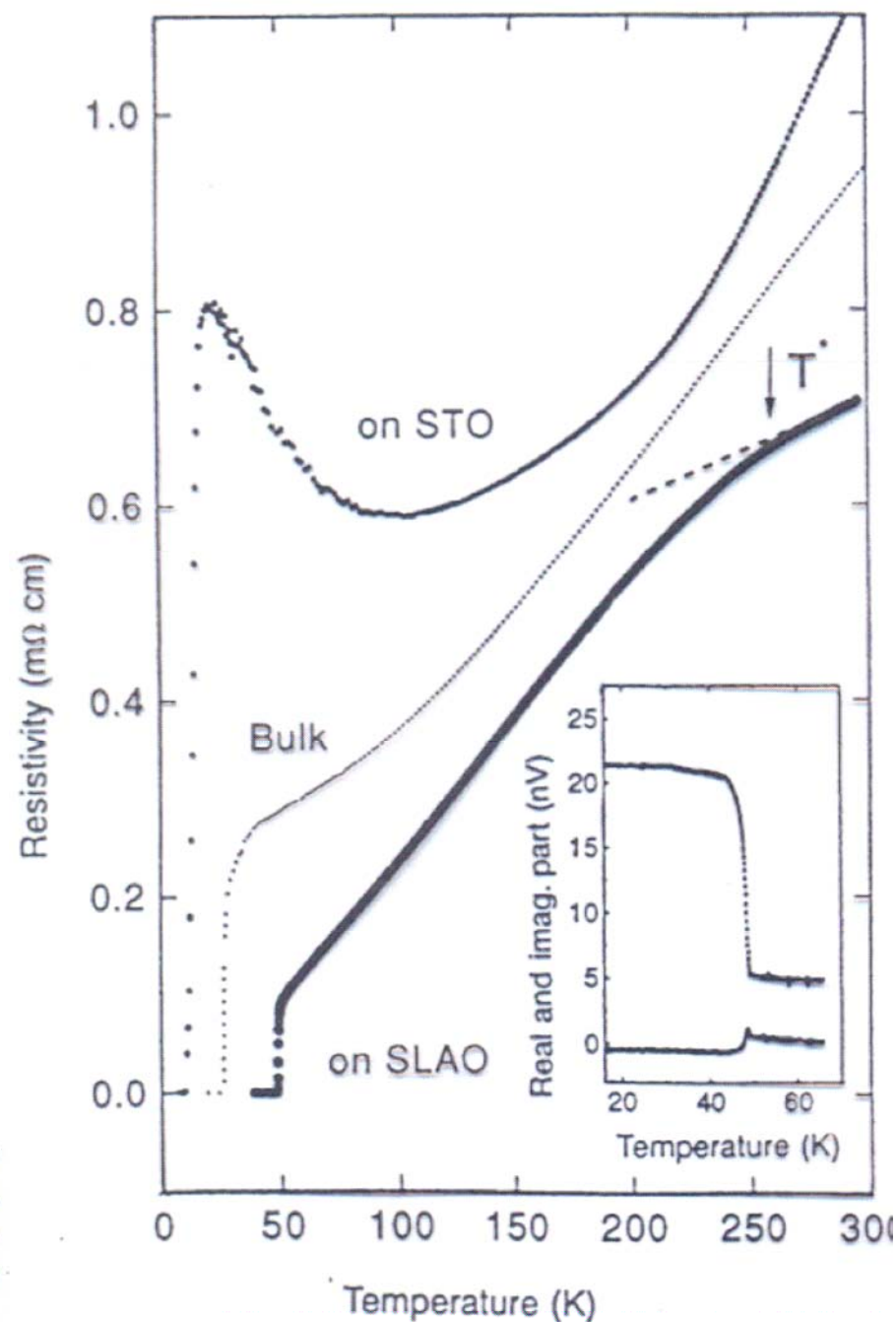
† Institut de Physique, Université de Neuchâtel, CH-2000 Neuchâtel, Switzerland

‡ Institute of Inorganic Chemistry, University of Bern, CH-3012 Bern, Switzerland

§ EMAT, RUCA, University of Antwerp, B-2020 Antwerpen, Belgium

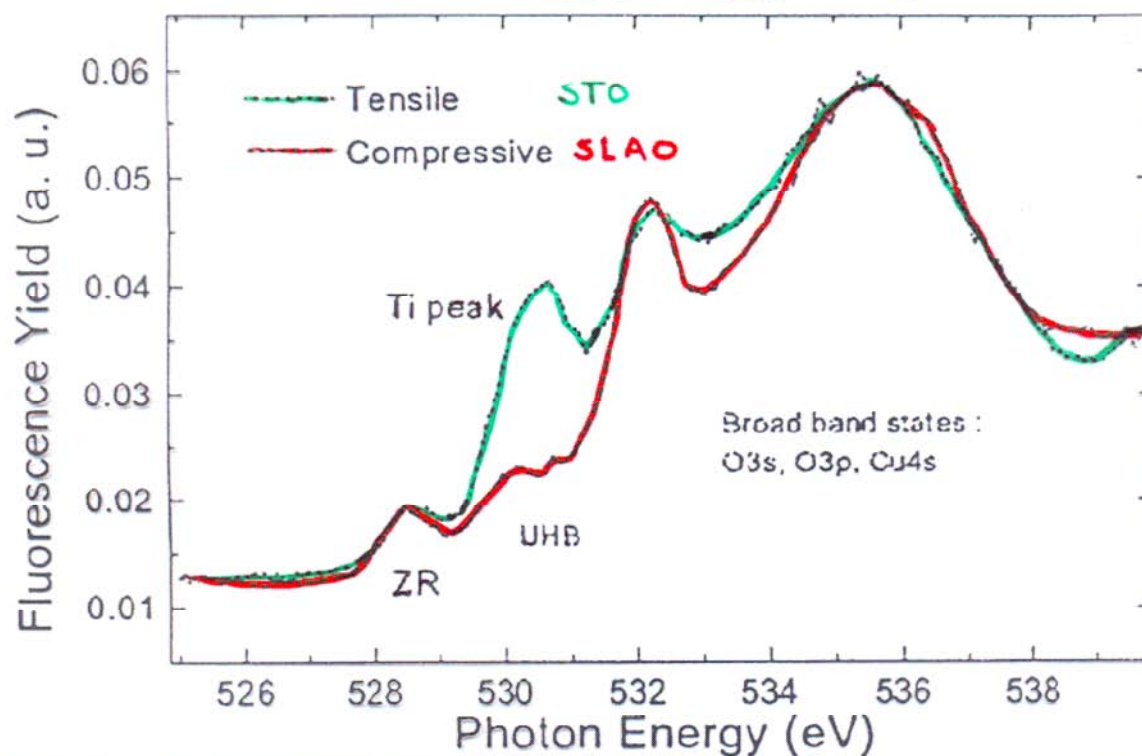
	$x = 0.10$	$x = 0.16$ (opt.)
STO	$T_c = 10\text{ K}$	
Bulk	$T_c = 25\text{ K}$	$T_c = 37\text{ K}$
SLAO	$T_c = 49\text{ K}$	

Figure 4 Resistivity versus temperature for the two films grown simultaneously and for the bulk $x = 0.10$ sample²⁶. Data were obtained using a four-point method. Inset, Real and imaginary parts of the a.c. susceptibility of the film on SLAO, which reveals a sharp, single-phase transition $\Delta T_c = 0.7\text{ K}$; the transition width of the film on STO is $\Delta T_c = 4\text{ K}$.



O-1s X-ray Absorption measurements (Tjeng, Abbamonte, Sawatzky)
ESRF - Feb '00

15 nm $\text{La}_{1.92}\text{Sr}_{0.08}\text{CuO}_4$



on STO and on SLAO : same oxygen hole concentration

$$x = 0.07$$

concentration from HALL-effect is not reliable !

Novel Electronic Properties on Ferroelectric / Ferro-magnetic Heterostructures

Hitoshi TABATA^{†(a)} and Tomoji KAWAI[†], Nonmembers

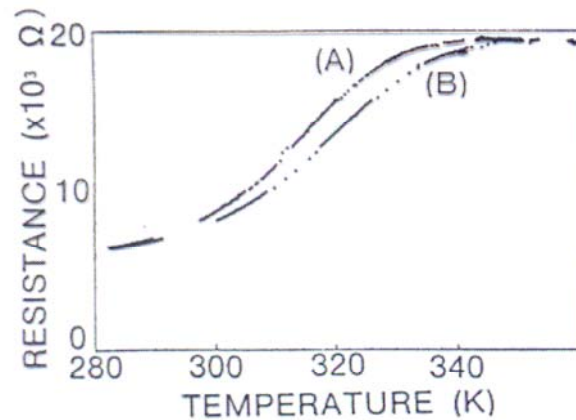
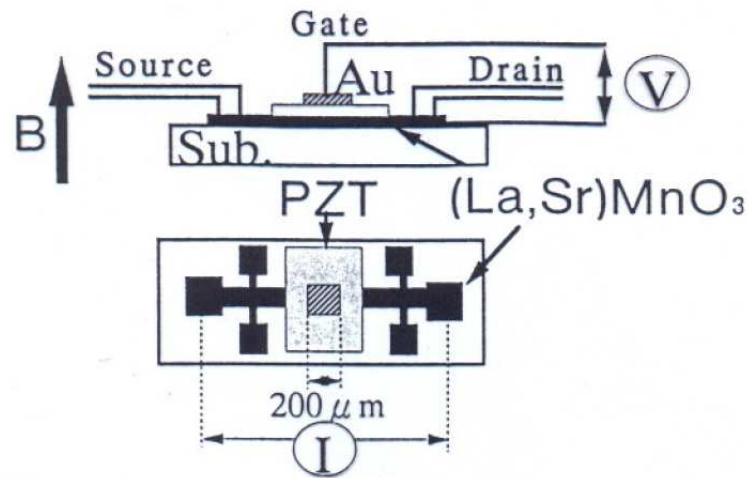


Fig. 7 Temperature vs. resistance of the (La, Sr) MnO₃ layer without (A) and with a gate voltage of 3 V (B).

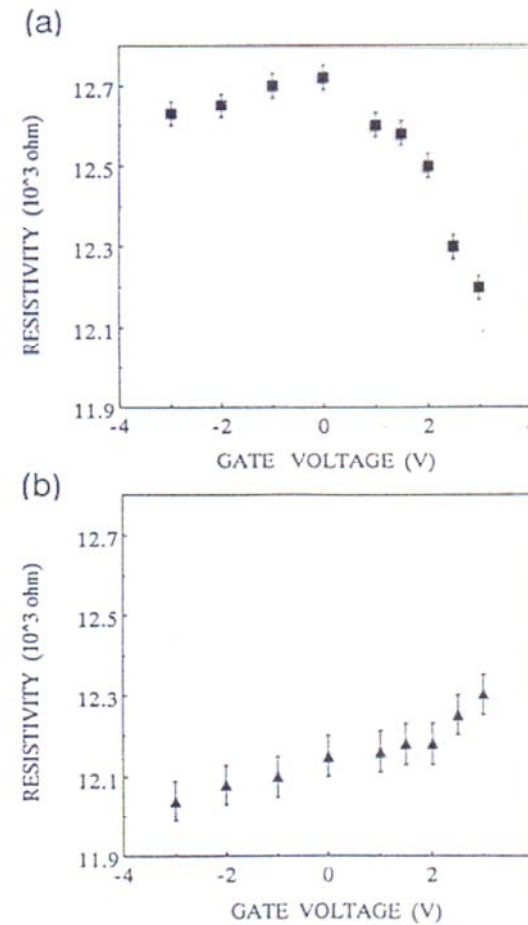


Fig. 8 Relation between the resistivity of ferroelectric LSMO layer and the gate voltage applied at a gate electrode (a) without magnetic field and (b) with magnetic field of 0.3 T (3000 G).

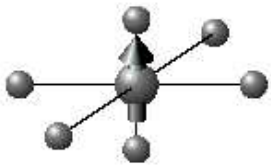
tensile in-plane strain

$$c/a < 1$$



(14Å)MnO/(10Å)CoO/(100Å)MnO/Ag(100)

$$\begin{aligned}\text{CoO} : a &= 4.424 \text{ \AA} \\ c &= 4.15 \text{ \AA}\end{aligned}$$

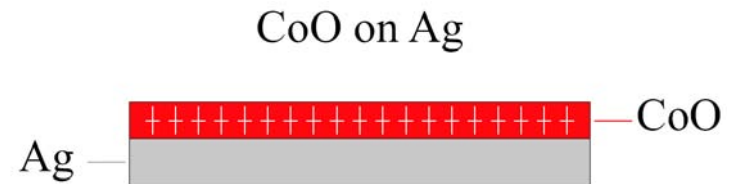


$$\begin{aligned}L_z &= 1.36 \mu_B \\ 2S_z &= 2.46 \mu_B\end{aligned}$$

anisotropy: +4.8 meV

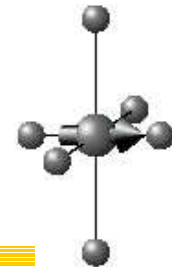
slightly compressive in-plane strain

$$c/a \gtrsim 1$$



(90Å)CoO/Ag(100)

$$\begin{aligned}\text{CoO} : a &= 4.235 \text{ \AA} \\ c &= 4.285 \text{ \AA}\end{aligned}$$



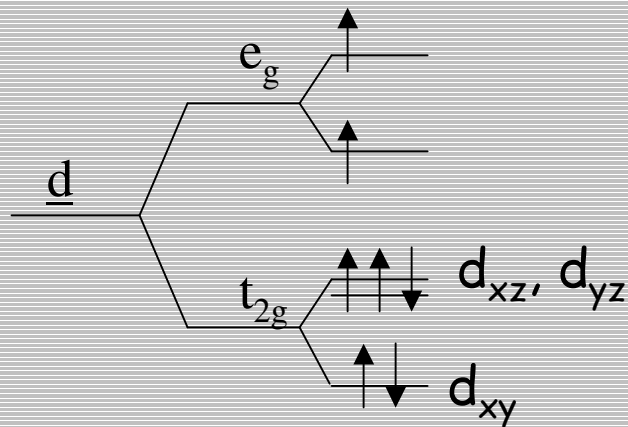
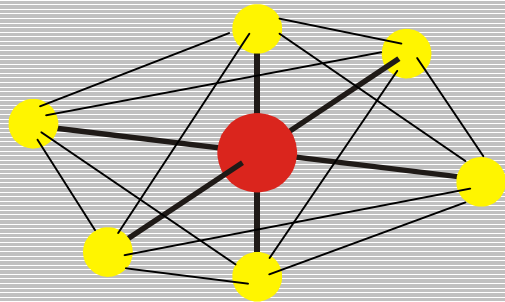
$$\begin{aligned}L_x &= 1.00 \mu_B \\ 2S_x &= 2.14 \mu_B\end{aligned}$$

anisotropy: - 1.6 meV

from best fit of
cluster calculations to
Co L_{23} XAS data

Orbital occupation and magnetic moment

CoO: high spin 3d⁷ ion



degenerate
real-space orbitals
 d_{yz}/d_{zx} -hole $\rightarrow d_{-1}$
 $L_z = 1 \mu_B$, $2S_z = 3 \mu_B$

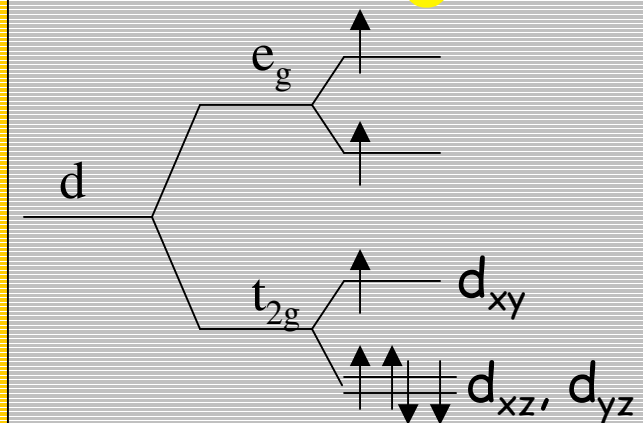
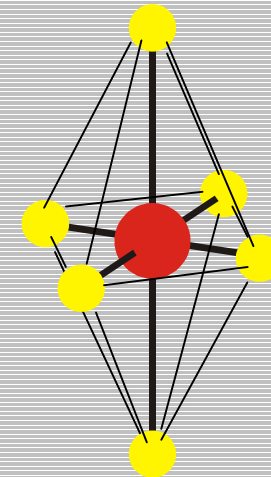
$$d_1 = \sqrt{\frac{1}{2}}(-id_{yz} - d_{zx})$$

$$d_{-1} = \sqrt{\frac{1}{2}}(-id_{yz} + d_{zx})$$

$$d_2 = \sqrt{\frac{1}{2}}(id_{xy} + d_{x^2-y^2})$$

$$d_{-2} = \sqrt{\frac{1}{2}}(-id_{xy} + d_{x^2-y^2})$$

$$d_0 = d_{z^2}$$



non-degenerate
real-space orbitals
 d_{xy} -hole
 $L_z = 0$, S in x-y plane

Can we use thin films to create new materials, new properties and new devices ?

Yes, but one needs to understand the 'physics', i.e. need to understand what happens to the electronic structure !

- Modification of material properties due to proximity of substrate:
 - strain
 - screening
 - charge donation
- New material compositions:
 - non-existent in bulk, but stabilized in film
- New sample preparation routes:
 - MBE combined with distillation and control of stoichiometry during growth by resistivity measurements

Ferromagnetism in LaFeO_3 - LaCrO_3 Superlattices

Science 280, 1064 (1998)

Kenji Ueda, Hitoshi Tabata, Tomoji Kawai*

Ferromagnetic spin order has been realized in the LaCrO_3 - LaFeO_3 superlattices. Ferromagnetic coupling between Fe^{3+} and Cr^{3+} through oxygen has long been expected on the basis of Anderson, Goodenough, and Kanamori rules. Despite many studies of Fe-O-Cr-based compounds, random positioning of Fe^{3+} and Cr^{3+} ions has frustrated the observation of ferromagnetic properties. By creating artificial superlattices of Fe^{3+} and Cr^{3+} layer along the $[111]$ direction, ferromagnetic ordering has been achieved.

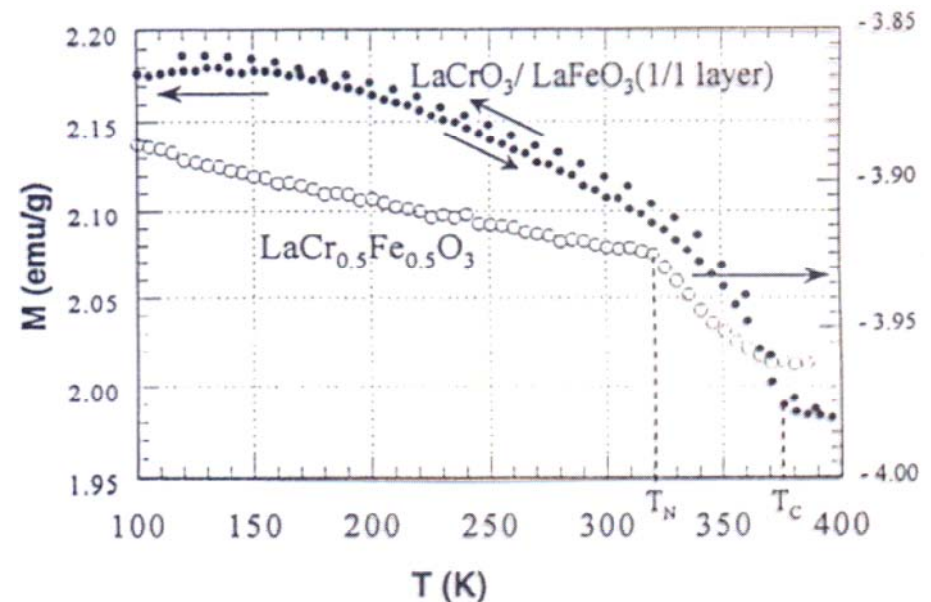
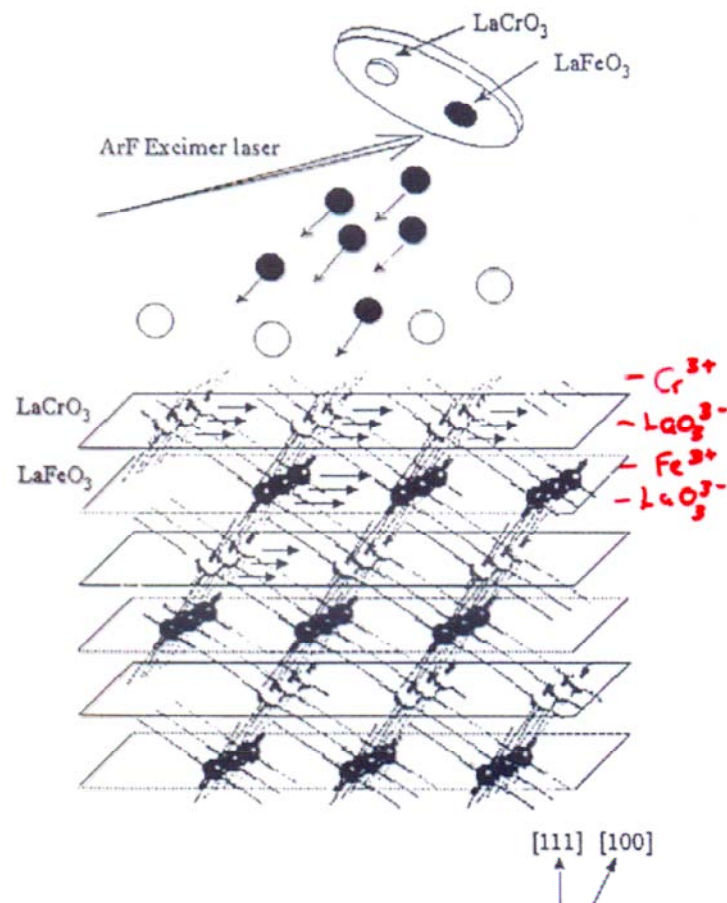
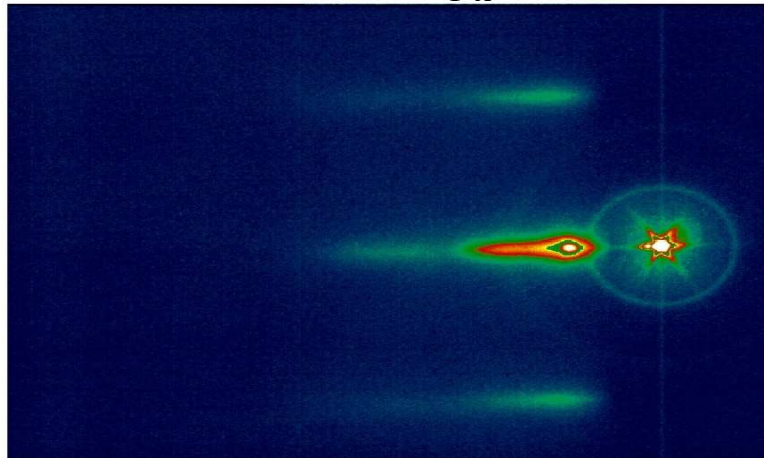


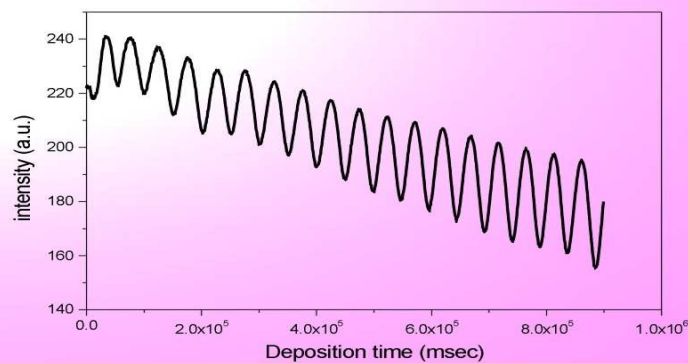
Fig. 3. Temperature dependence of magnetization of LaCrO_3 - LaFeO_3 superlattice on SrTiO_3 (111) (●) and that of $\text{LaCr}_{0.5}\text{Fe}_{0.5}\text{O}_3$ solid solution film (○), measured in a 0.1-T magnetic field applied parallel to the substrate surface.

Stabilizing rocksalt Cr_{1-x}O by epitaxial growth

RHEED on 18 ML Cr_{1-x}O on $\text{MgO}(100)$



RHEED intensity vs. deposition time



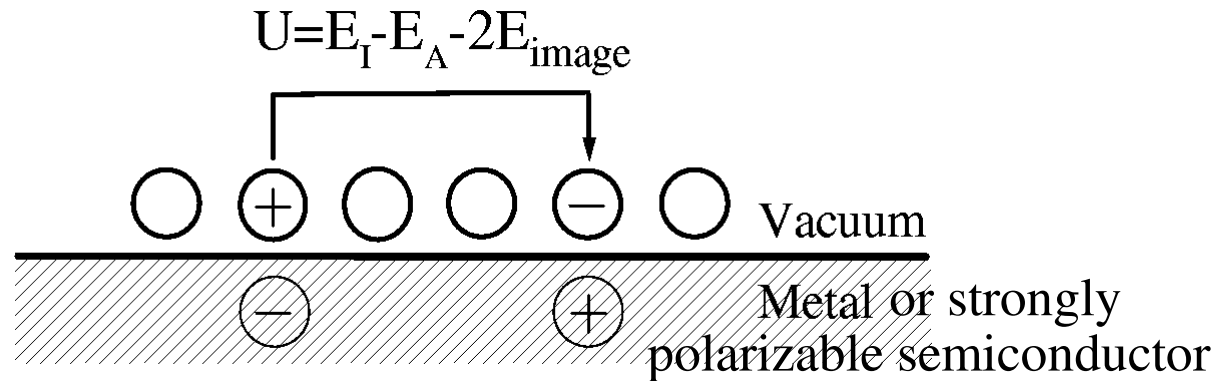
- $0 < x < 0.3$
- defect structure (ordered)
- multilayers $\text{Cr}_{1-x}\text{O}/\text{MgO}$
- with NO_2 : $\text{CrO}_{2/3}\text{N}_{1/3}$?!

Can we use thin films to create new materials, new properties and new devices ?

Yes, but one needs to understand the 'physics', i.e. need to understand what happens to the electronic structure !

- Modification of material properties due to proximity of substrate:
 - strain
 - screening
 - charge donation
- New material compositions:
non-existent in bulk, but stabilized in film
- New sample preparation routes:
MBE combined with distillation and
control of stoichiometry during growth by resistivity measurements

Modification of material properties using image charge screening



Reduction of charge excitation energies:

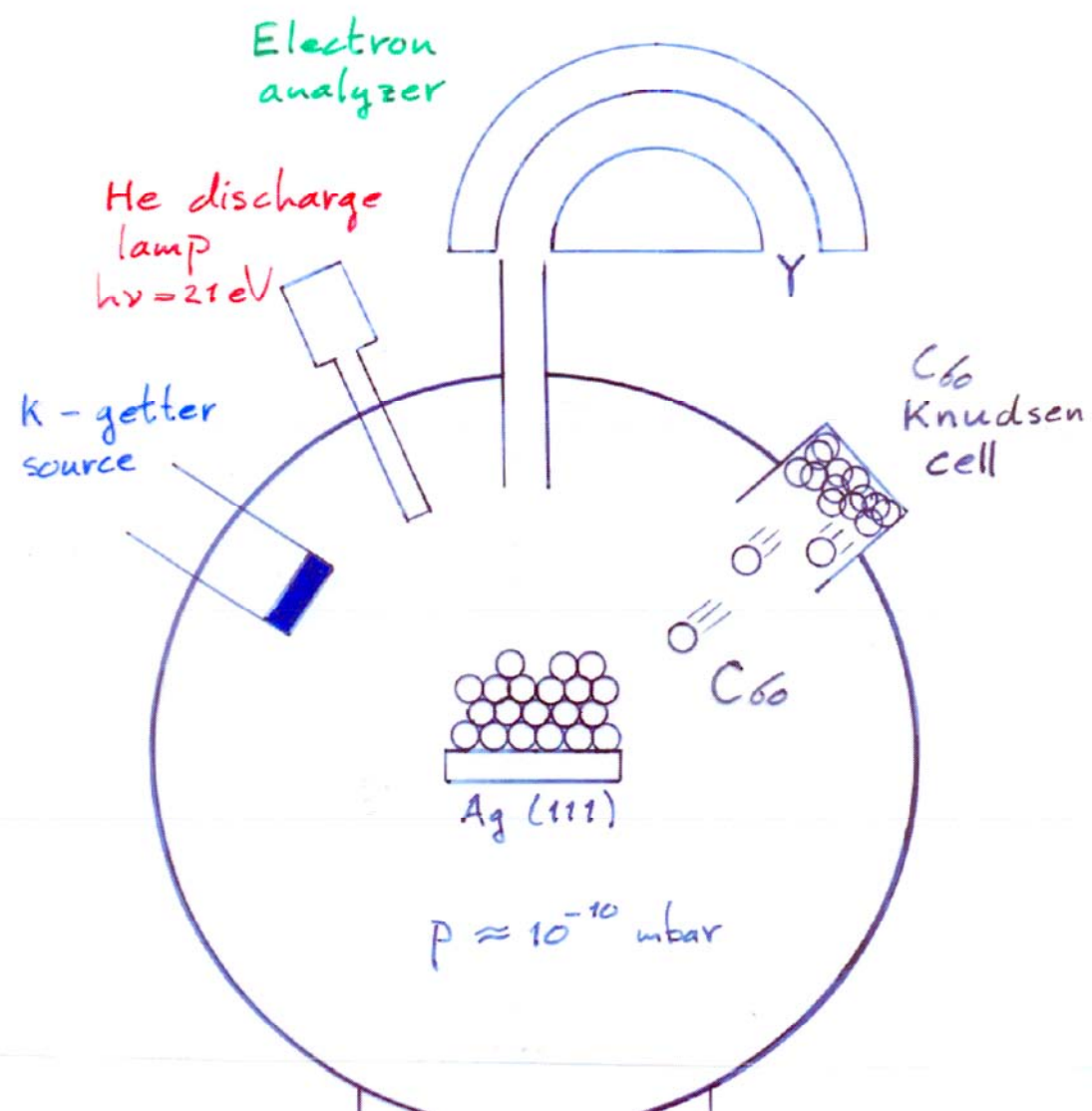
- Coulomb energy: $U = U_o - 2E_{\text{image}}$
- Charge transfer energy: $\Delta = \Delta_o - 2E_{\text{image}}$
- Bandgap: $E_g = E_{go} - 2E_{\text{image}}$

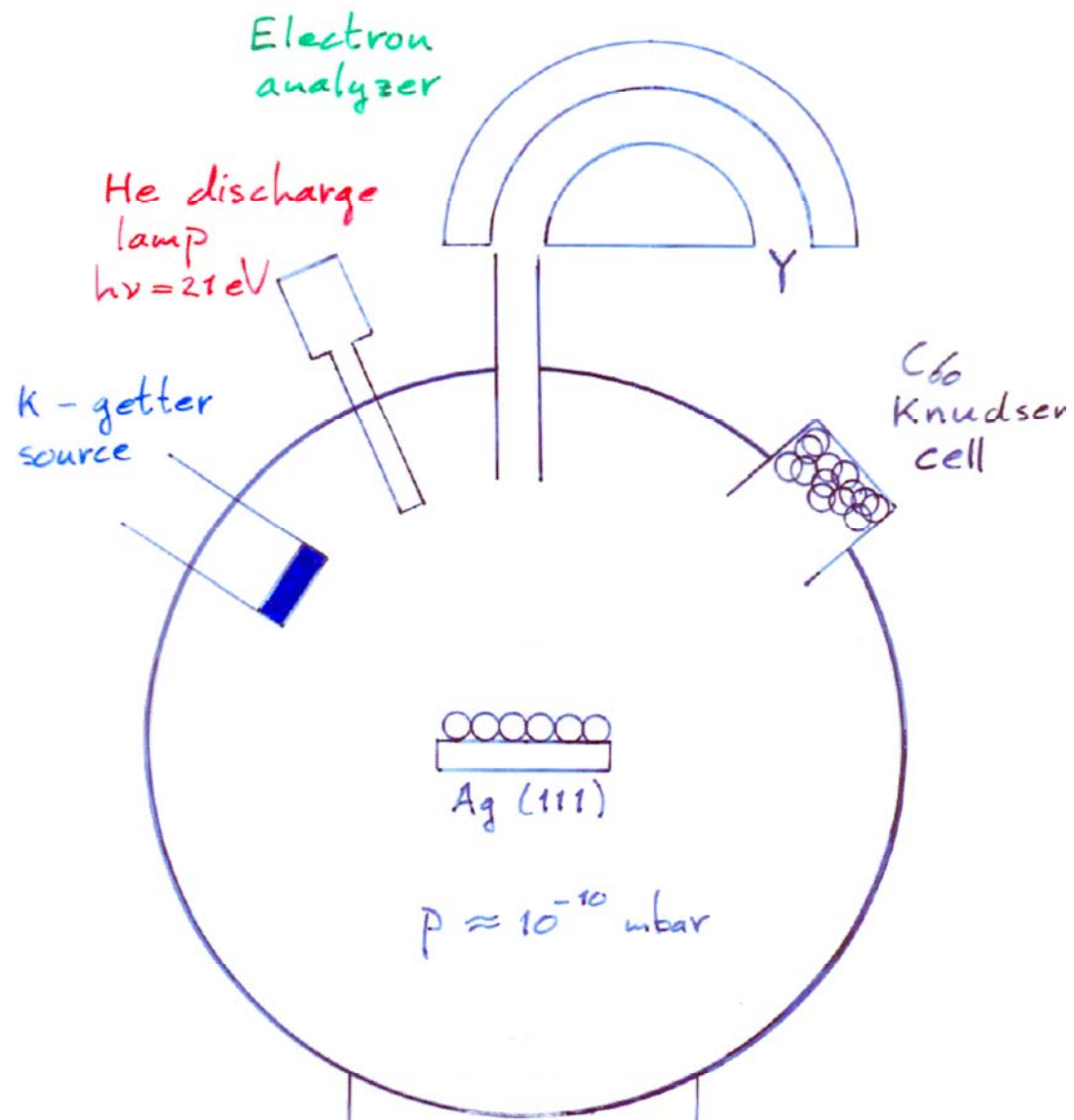
Examples from experiments:

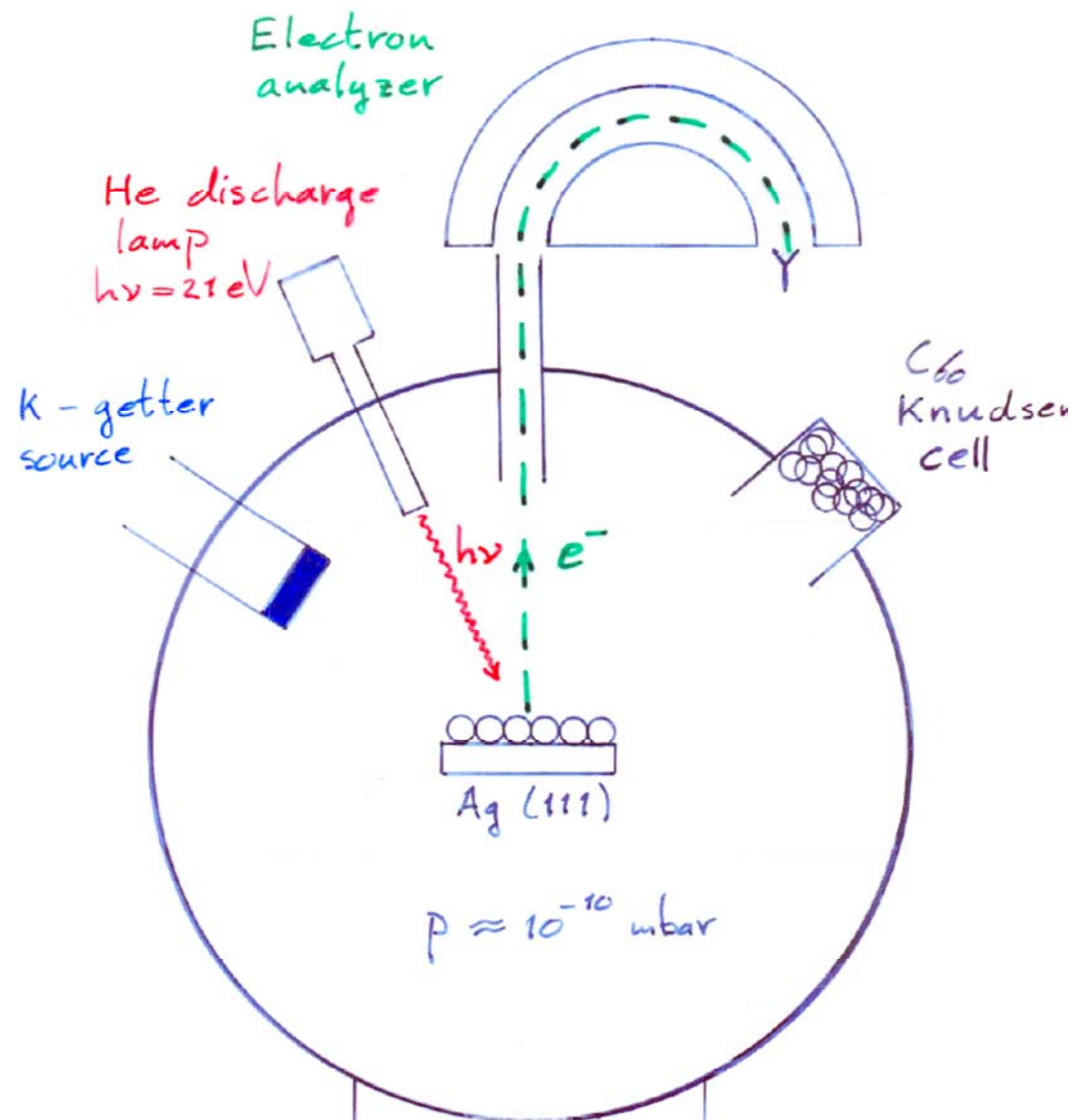
- Monolayer C_{60} on Ag : U and E_g reduced by 1 eV
- thin oxide film on Ag : U and Δ reduced by 1-2 eV

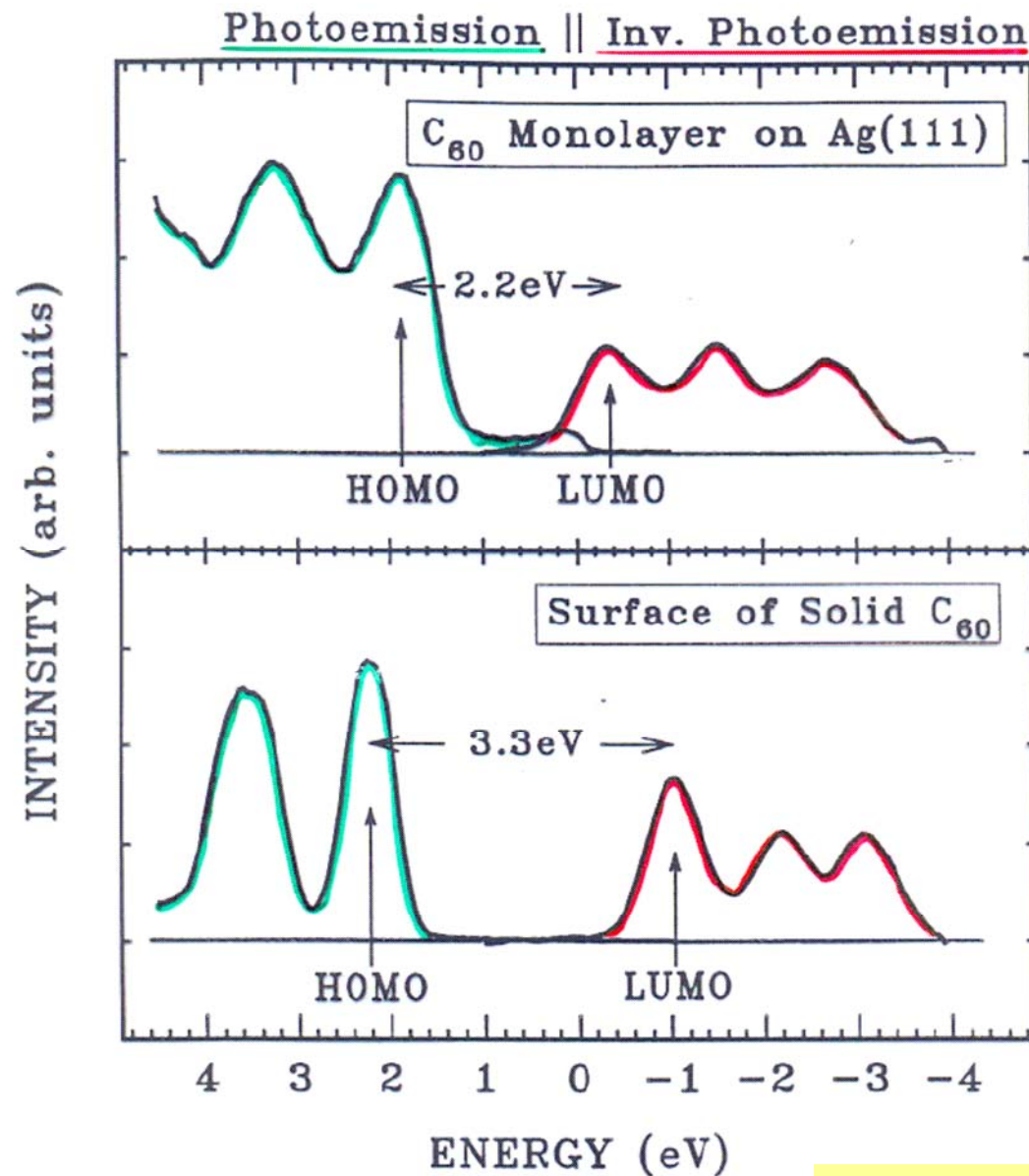
Expectations:

- Stronger (super)exchange interactions: $\sim t^2/U$; $\sim t^4/\Delta^2(1/U - 1/\Delta)$
- Higher T_C and T_N ?!!





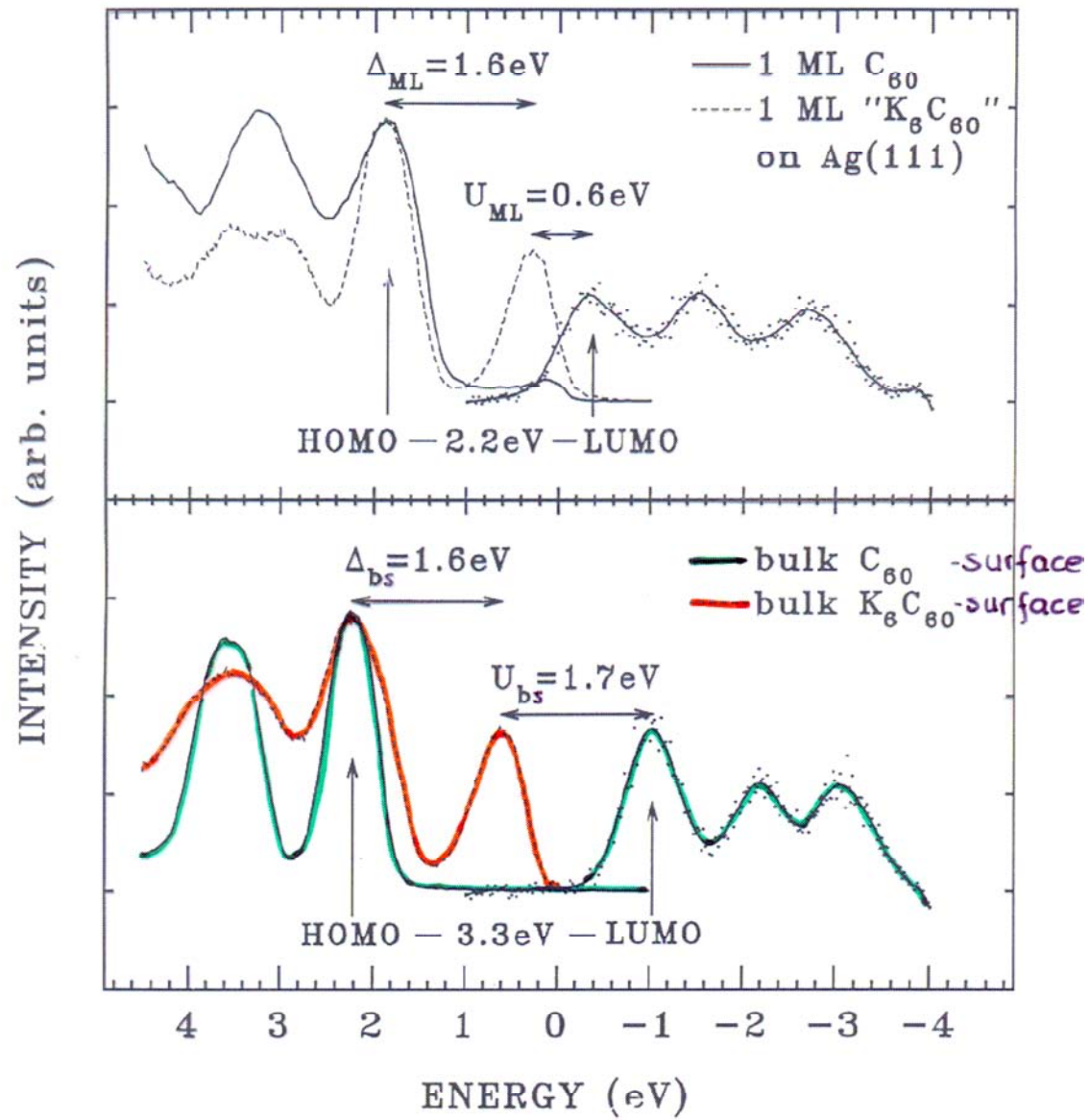




Bandgap is reduced!
Molecular orbital structure is conserved!

Rigidly!

MgO monolayer on Ag(100):
U and Δ reduced by 2 eV!
Multiplet splittings are conserved!



Bandgap is reduced because on-site Coulomb energy U is reduced!

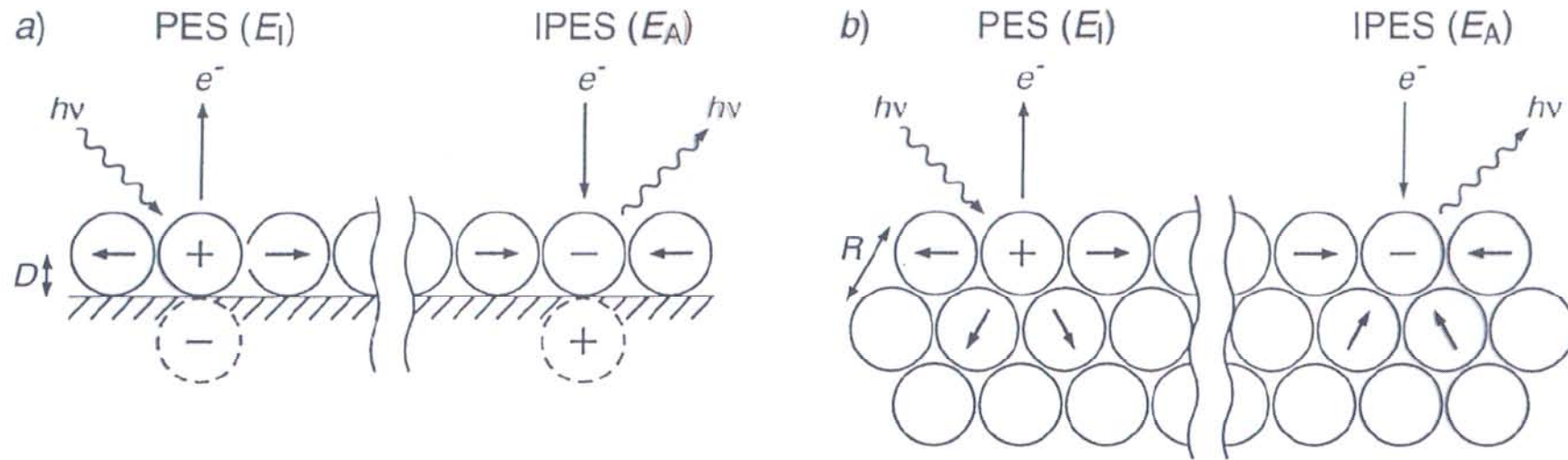


Fig. 3. – Photoemission and inverse photoemission processes for a monolayer of C₆₀ on metal (a) and for the surface of bulk C₆₀ (b). In both cases, the final state charges and polarizations of the bucky-balls are indicated.

$$E_g = E_g^{at} - 2E_p(C_{60}) - 2E_p(\text{metal})$$

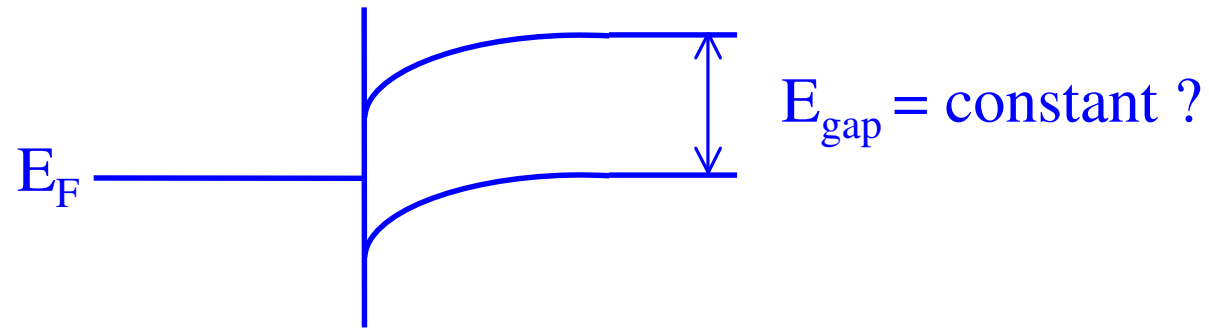
$$\begin{array}{ccccccc} \downarrow & \downarrow & \downarrow & \vdots & & & \\ 2.2 \text{ eV} & 5.0 \text{ eV} & 1.2 \text{ eV} & \rightarrow & 1.6 \text{ eV} & & \\ & & \text{(6 nearest neighbors)} & & & & \end{array}$$

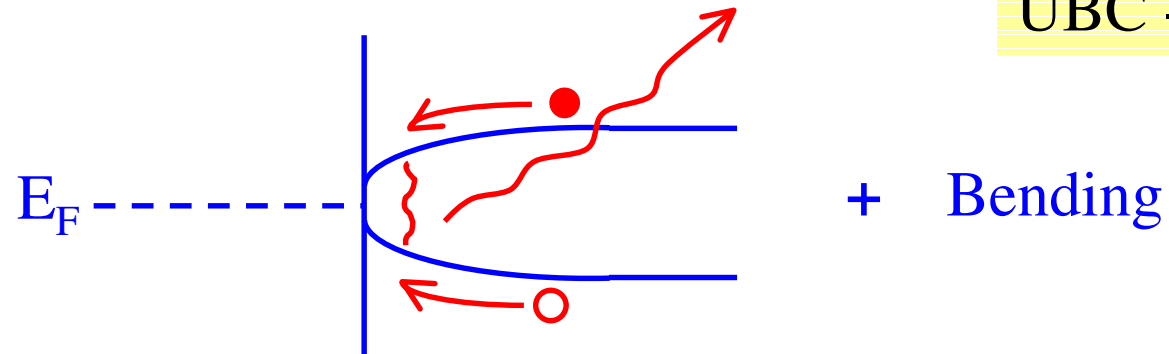
$$E_g = E_g^{at} - 2E_p(C_{60})$$

$$\begin{array}{ccccccc} \downarrow & \downarrow & \vdots & & & & \\ 3.3 \text{ eV} & 5.0 \text{ eV} & \rightarrow & 1.7 \text{ eV} & & & \\ & & \text{(9 nearest neighbors)} & & & & \end{array}$$

$$2E_p(\text{metal} = \text{image charge}) = \frac{e^2}{2D} = 1.44 \text{ eV} \quad (D \approx 5 \text{ \AA})$$

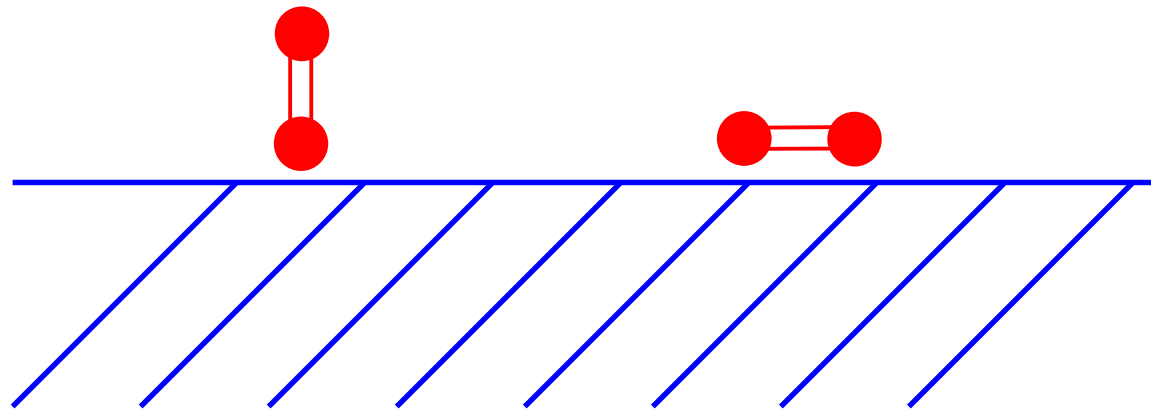
What happens at a semiconductor –metal interface





$$\Delta E_{\text{gap}} \sim 1\text{eV}$$

Depends on Orientation!



Orientation changes the gap at interface
Orientation disorder is really bad

Influence of STM tip on
bandgap of solid C₆₀ ?!

Can we use thin films to create new materials, new properties and new devices ?

Yes, but one needs to understand the 'physics', i.e. need to understand what happens to the electronic structure !

- Modification of material properties due to proximity of substrate:

- strain
- screening

- charge donation

- New material compositions:

- non-existent in bulk, but stabilized in film

- New sample preparation routes:

- MBE combined with distillation and control of stoichiometry during growth by resistivity measurements

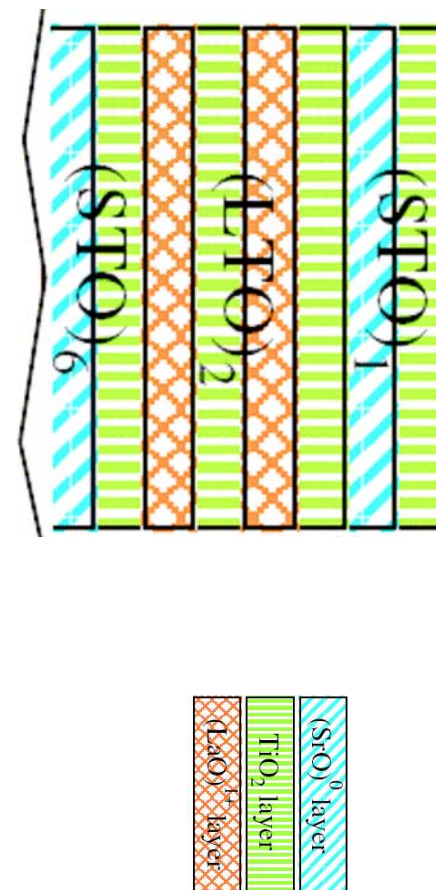
Electronic reconstruction at an interface between a Mott insulator and a band insulator

NATURE | VOL 428 | 8 APRIL 2004 | 630

Satoshi Okamoto & Andrew J. Millis

Department of Physics, Columbia University 538 West 120th Street, New York, New York 10027, USA

Surface science is an important and well-established branch of materials science involving the study of changes in material properties near a surface or interface. A fundamental issue has been atomic reconstruction: how the surface lattice symmetry differs from the bulk. ‘Correlated-electron compounds’ are materials in which strong electron–electron and electron–lattice interactions produce new electronic phases, including interaction-induced (Mott) insulators, many forms of spin, charge and orbital ordering, and (presumably) high-transition-temperature superconductivity^{1,2}. Here we propose that the fundamental issue for the new field of correlated-electron surface/interface science is ‘electronic reconstruction’: how does the surface/interface electronic phase differ from that in the bulk? As a step towards a general understanding of such phenomena, we present a theoretical study of an interface between a strongly correlated Mott insulator and a band insulator. We find dramatic interface-induced electronic reconstructions: in wide parameter



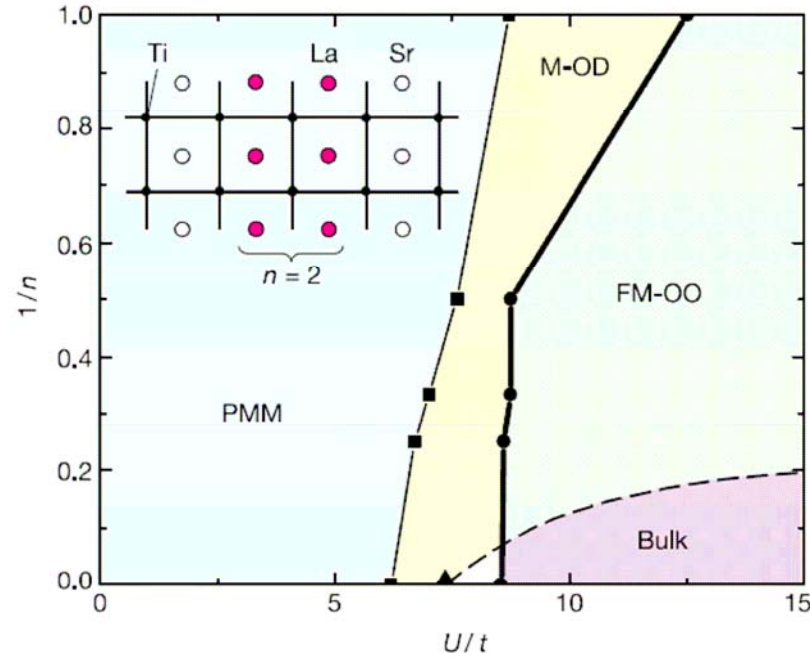


Figure 1 Ground-state phase diagram computed in Hartree–Fock approximation as a function of the on-site Coulomb interaction U and the inverse of the La layer number n . For small U values the ground state is a paramagnetic metal with no orbital ordering (PMM region; shaded blue). The solid line marked with squares denotes a second-order transition to a orbitally disordered magnetic state (M-OD; shaded yellow) that is ferromagnetic for $n = 1$; for $n > 1$ each (001) Ti layer is uniformly polarized, but the magnetization direction alternates from layer to layer, leading to a ferrimagnetic state ($n = 2, 4, 6, \dots$; odd number of occupied Ti layers) or antiferromagnetic state ($n = 3, 5, 7, \dots$; even number of occupied Ti layers). The solid line marked with circles denotes a first-order transition to a fully polarized ferromagnetic state with (00 π) orbital order (FM-OO; shaded green). For sufficiently thick samples (Bulk, shaded pink), the latter transition is pre-empted by a first-order transition to the bulk state, which, in the Hartree–Fock approximation used here, has ferromagnetic spin order and G -type ($\pi\pi\pi$) antiferro-orbital order. The actual materials exhibit a G -type AF order and a complicated orbital order²⁰ apparently due to subtle lattice distortions neglected here²¹. Inset, schematic of plane perpendicular to (010) direction of (001) superlattice for the $n = 2$ case. Circles show the positions of Sr (white) and La (red) ions respectively; small black dots show the positions of Ti ions.

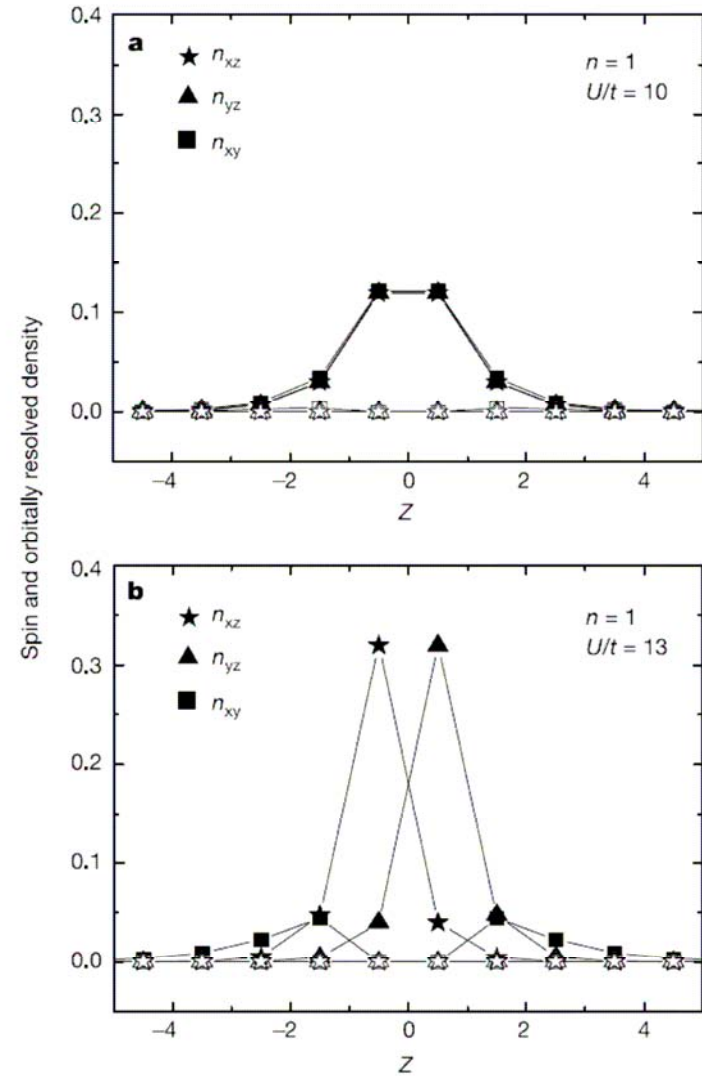


Figure 2 Spin and orbitally resolved charge densities as function of transverse (001) coordinate z for heterostructure with one La layer. La plane is at $z = 0$. Filled (open) symbols indicate majority (minority) spin densities for xz , yz and xy orbitals (see key on figure). **a**, Intermediate U (M-OD) regime; full spin polarization but all three orbitals equally occupied. **b**, Large U (FM-OO) regime. Full spin polarization persists, orbital disproportionation occurs. In the Ti layer at $z = 1/2$, the yz orbital is dominant; in the Ti layer at $z = -1/2$, the xz orbital is dominant; at larger $|z|$ the xy orbital is dominant, but the electron density is low.

ranges, the near-interface region is metallic and ferromagnetic, whereas the bulk phase on either side is insulating and anti-ferromagnetic. Extending the analysis to a wider range of interfaces and surfaces is a fundamental scientific challenge and may lead to new applications for correlated electron materials.

To assess the effects of a surface or interface on correlated-electron behaviour we require to understand the changes in the parameters governing bulk correlated-electron behaviour. The three key factors are interaction strengths, bandwidths and electron densities^{1,3}, all of which may change near a surface or interface. In most cases, surface- or interface-induced changes in all three factors will contribute, but in developing a general understanding it is desirable first to study the different effects in isolation. Here we focus on the effect of electron-density variation caused by the spreading of charge across an interface. A different charge distribution effect—the compensation of a polar surface by electronic charge rearrangement—was argued to change the behaviour of C₆₀ films⁴. (Indeed, Hesper *et al.*⁴ coined the term “electronic reconstruction” in reference to this specific effect; we suggest that this useful phrase be applied more generally to denote electronic phase behaviour that is fundamentally different at a surface from in bulk.) Proximity to a surface or interface can also change the electron interaction parameters^{5,6}, the electron bandwidth⁷, and level degeneracy⁸. Experimental studies of surfaces^{9–12} and heterostructures¹³

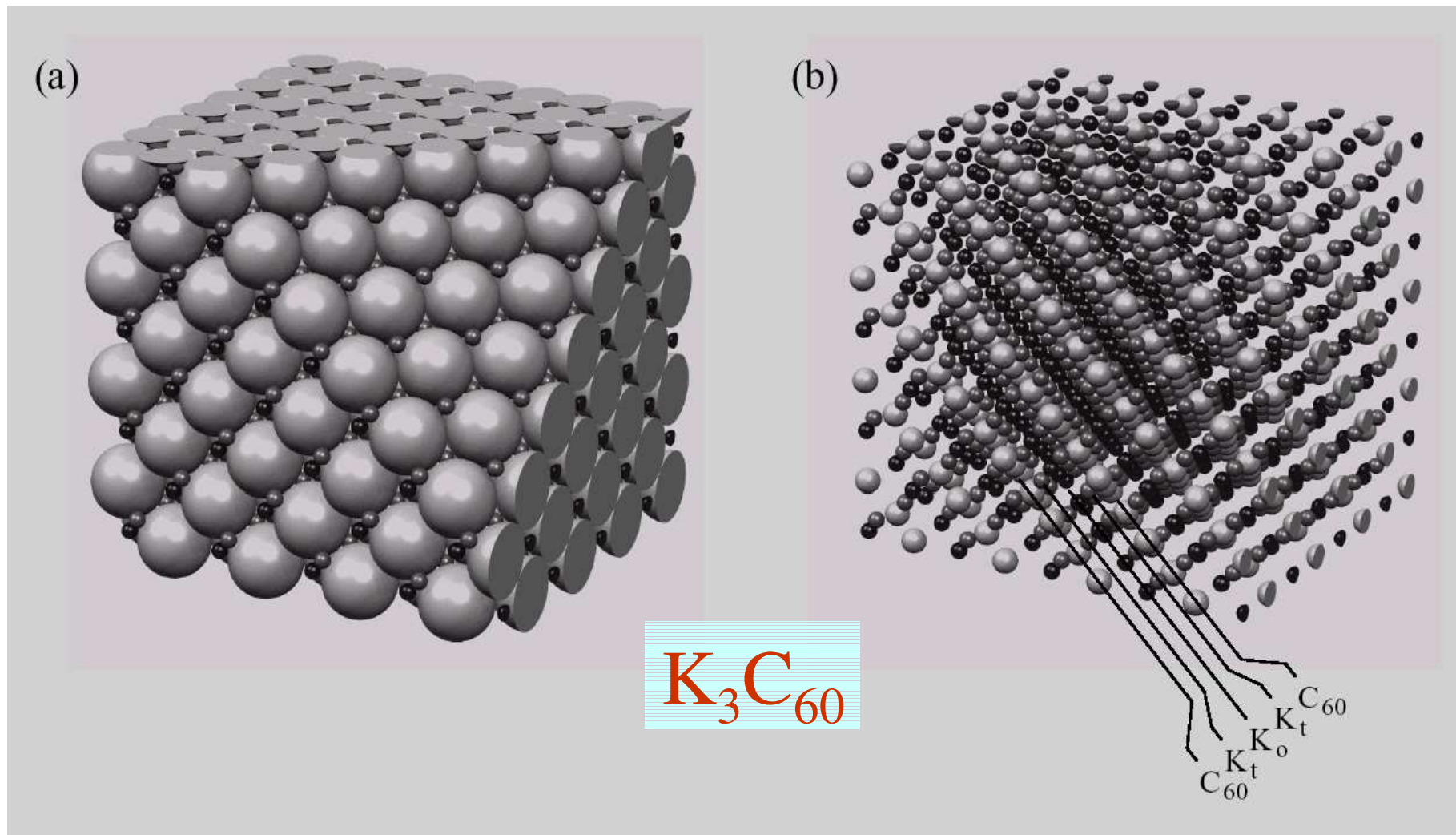
4. Hesper, R., Tjeng, L. H., Heeres, A. & Sawatzky, G. A. Photoemission evidence of electronic stabilization of polar surface in K₃C₆₀. *Phys. Rev. B* **62**, 16046–16055 (2000).
6. Altieri, S., Tjeng, L. H. & Sawatzky, G. A. Electronic structure and chemical reactivity of oxide-metal interfaces: MgO(100)/Ag(100). *Phys. Rev. B* **61**, 16948–16955 (2000).

Photoemission evidence of electronic stabilization of polar surfaces in K_3C_{60}

R. Hesper, L. H. Tjeng, A. Heeres, and G. A. Sawatzky

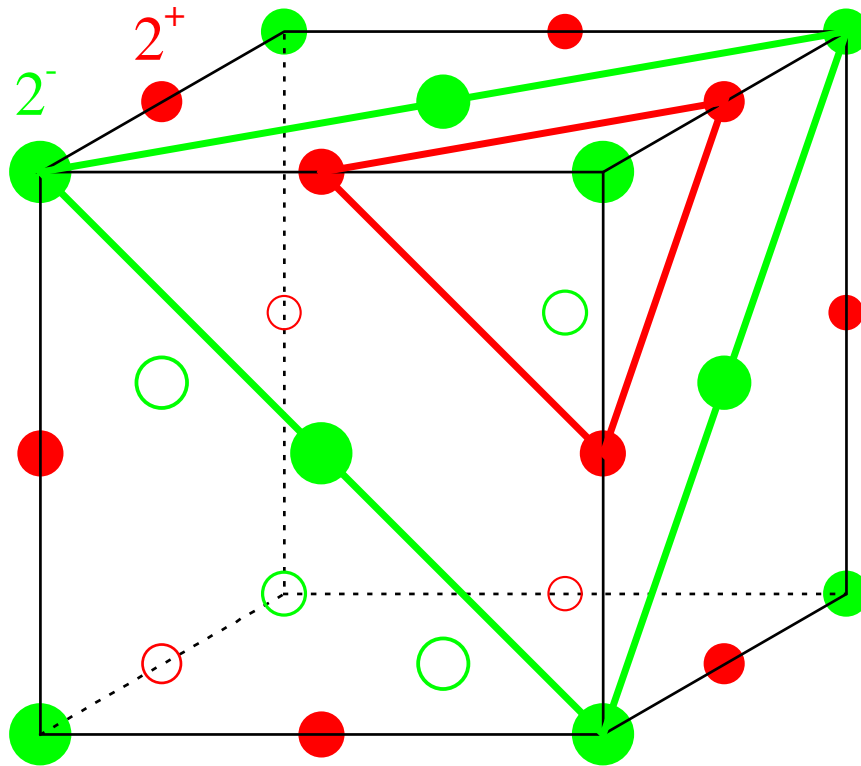
Solid State Physics Laboratory, Materials Science Centre, University of Groningen, Nijenborgh 4, 9747 AG Groningen, the Netherlands

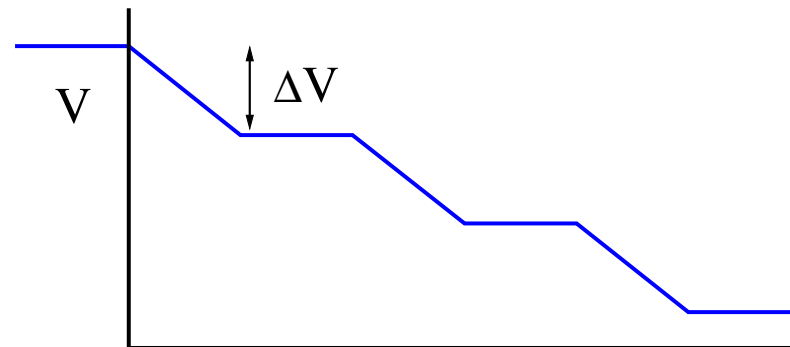
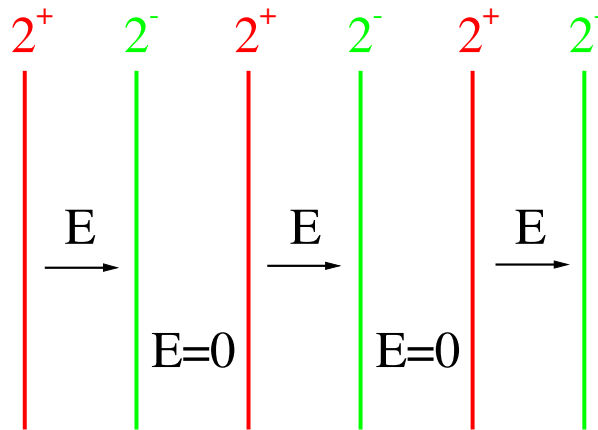
(Received 19 April 2000)



Polar Surfaces

- Existence of non-neutral or charged planes in crystal structures
- Rocksalt (111) surfaces: MgO , NiO

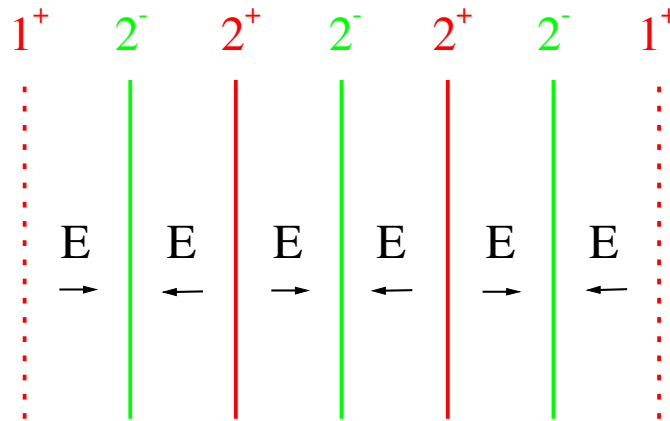




$\Delta V = 57.9 \text{ Volt}$ per MgO or NiO double layer

IMPOSSIBLE !!

half charge termination



half charge termination



Surface

- facets: pyramids with (100) surfaces
- reconstructs: octopolar at NiO (111)
- attracts charged contaminants: OH^- , I^- Surfactants !!
- Zener-breakdown: ionic charge at surface \neq in bulk

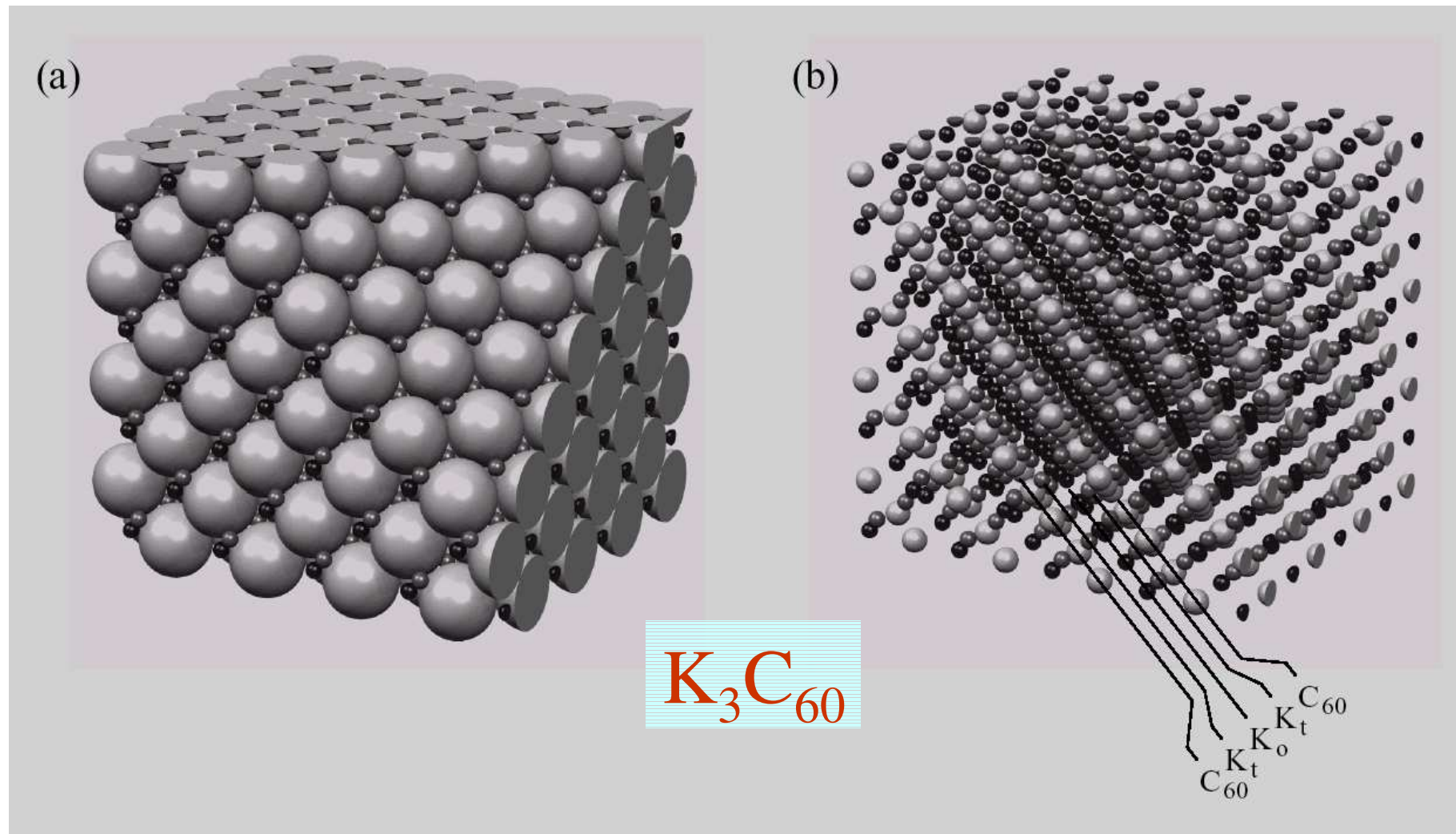
MnS(111): I^-
 ZnO(0001): OH^- , Na^+
 MgO(111) in Cu
 K_3C_{60} (111): $\text{C}_{60}^{1.5-}$
 EuO(111): Eu^{1+}

Photoemission evidence of electronic stabilization of polar surfaces in K_3C_{60}

R. Hesper, L. H. Tjeng, A. Heeres, and G. A. Sawatzky

Solid State Physics Laboratory, Materials Science Centre, University of Groningen, Nijenborgh 4, 9747 AG Groningen, the Netherlands

(Received 19 April 2000)



insulator

ALKALI METAL FULLERIDES

Superconductors

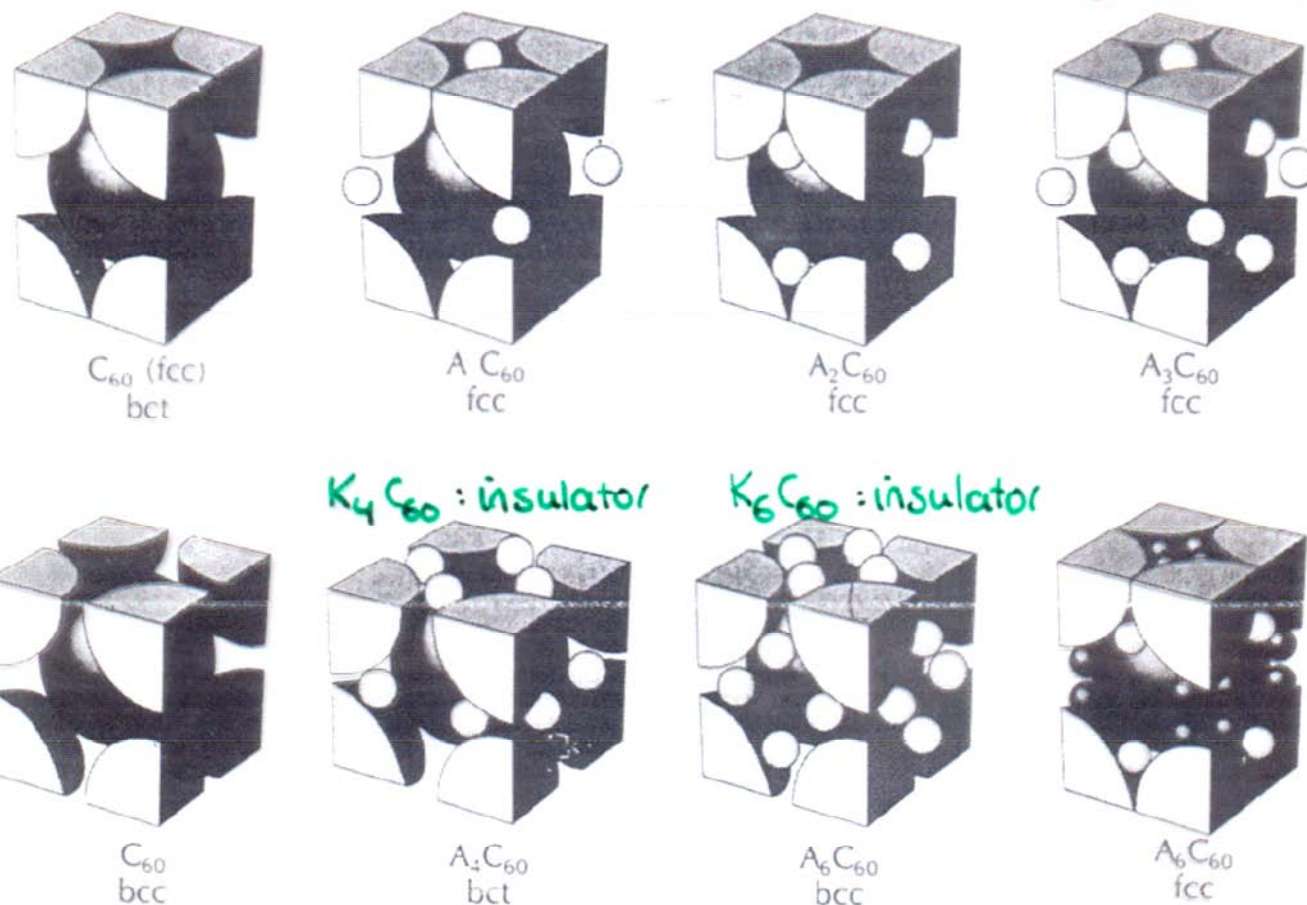
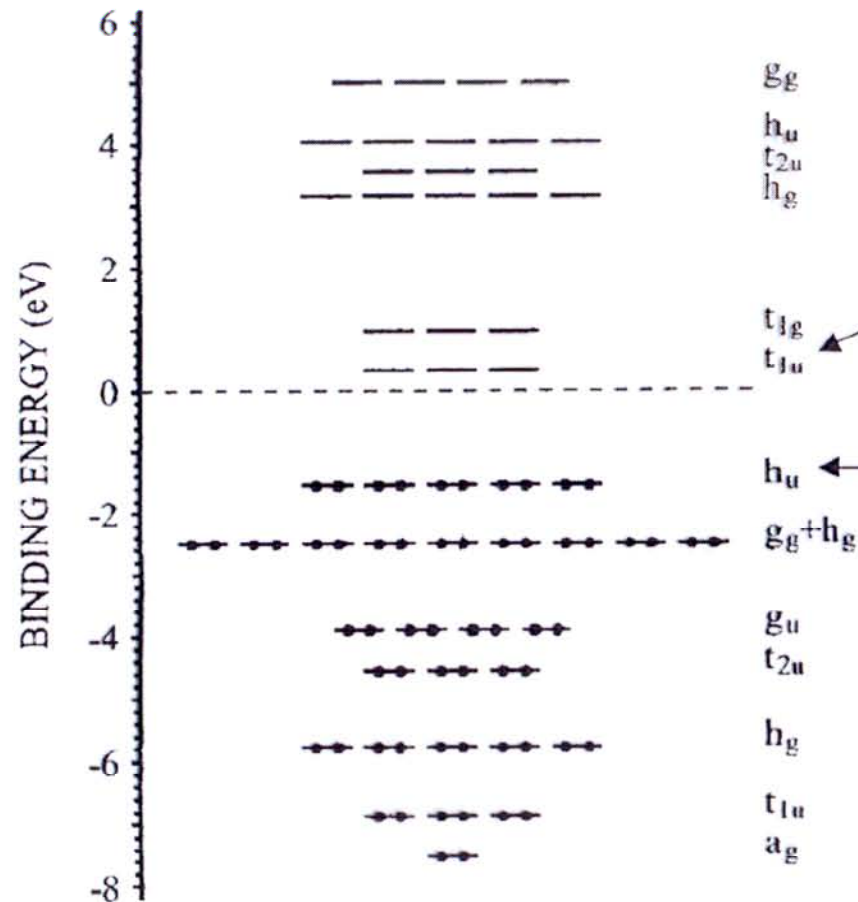
 $K_3C_{60} : T_c = 19\text{ K}$ $Rb_3C_{60} : T_c = 30\text{ K}$ 

FIG. 21. The crystal structures of the fulleride family. The top row shows the fcc structure of undoped C_{60} , the A_1C_{60} structure with octahedral site occupancy, the A_2C_{60} structure with tetrahedral site occupancy, and the A_3C_{60} structure with tetrahedral and octahedral site occupancy. The bottom row shows C_{60} molecules arranged in the bcc structure, the filling of tetrahedral sites producing A_4C_{60} and A_6C_{60} . The bottom-right structure corresponds to

Elektronische Struktur eines C_{60} Moleküls



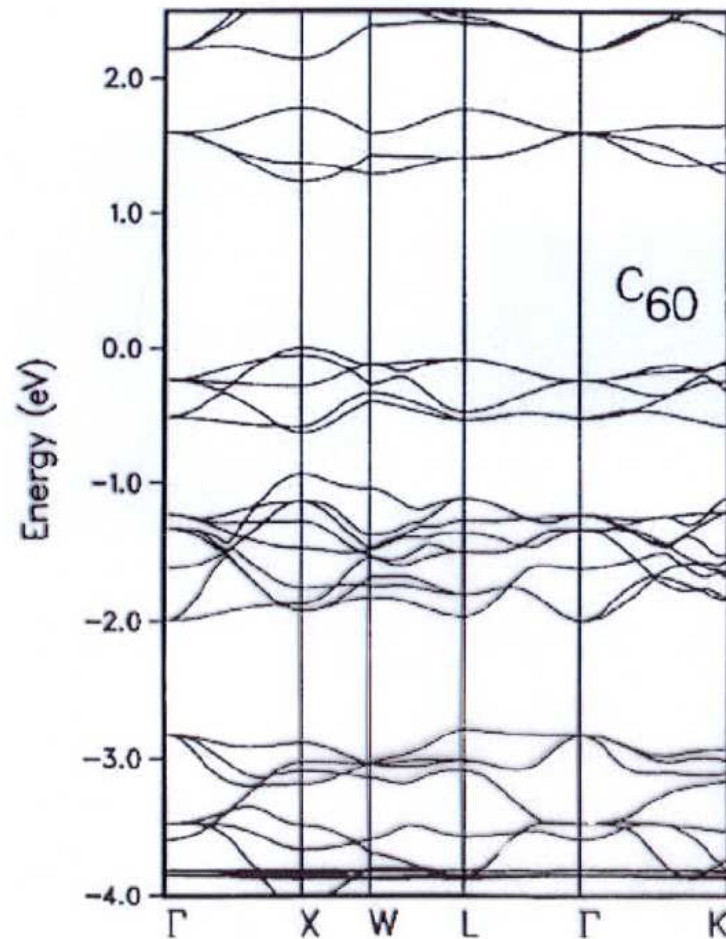
- t_{1u} Orbital ist LUMO
(Lowest Unoccupied
Molecular Orbital)

- h_u Orbital ist HOMO
(Highest Occupied
Molecular Orbital)

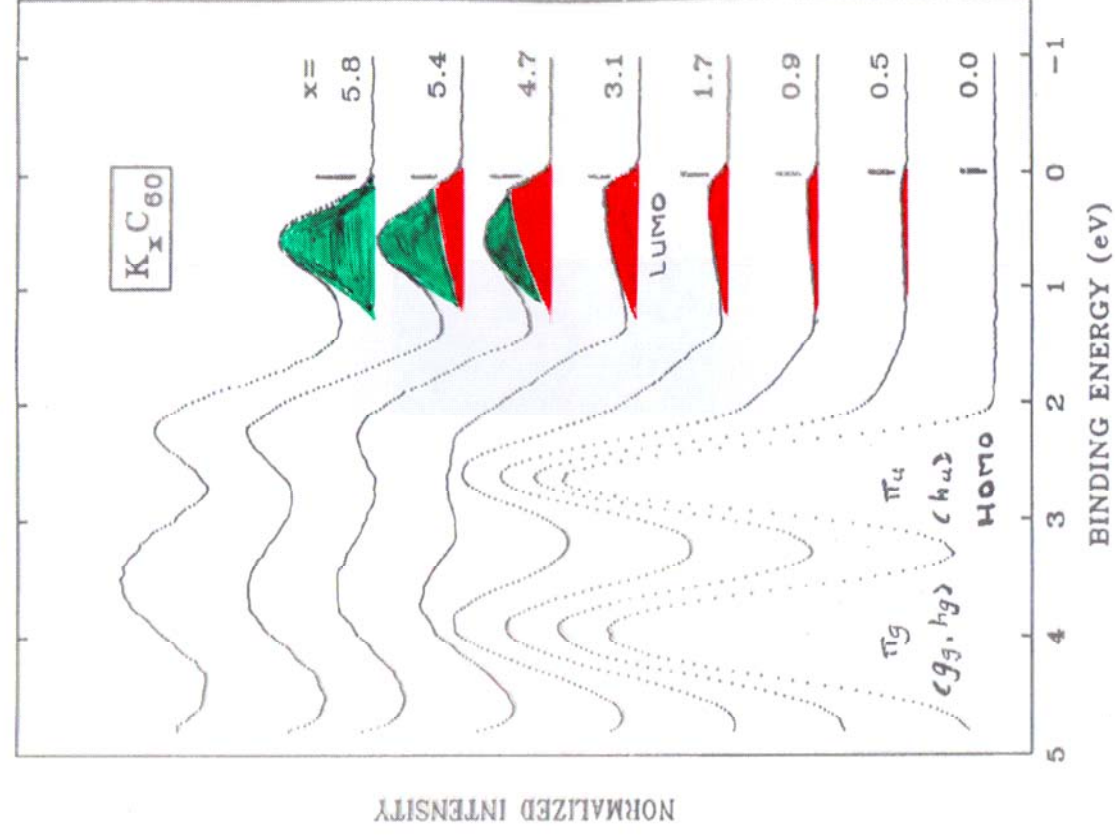
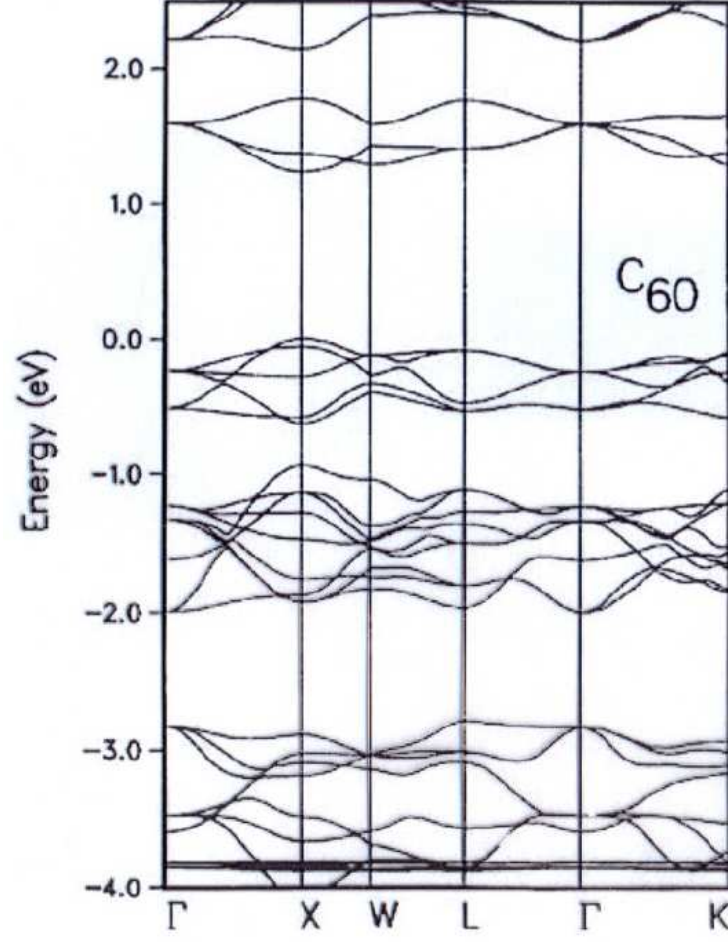
- HOMO vollständig gefüllt

Bandstruktur eines C_{60} Festkörpers

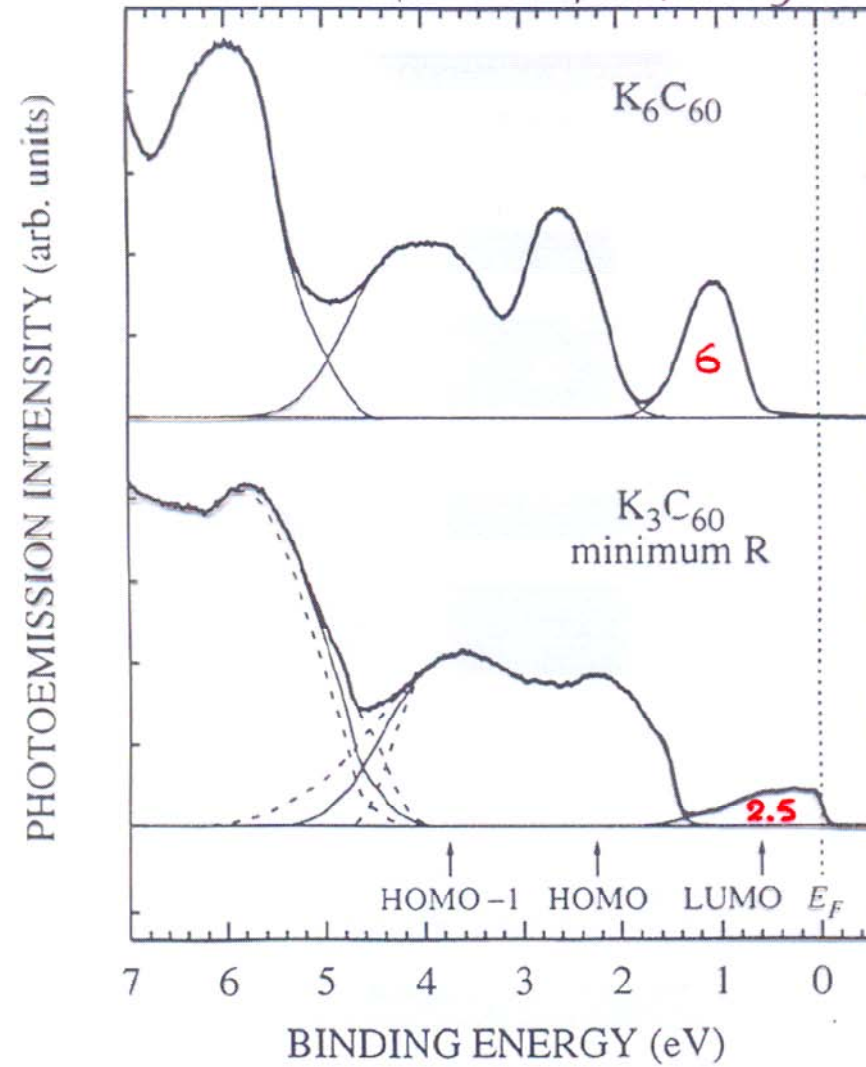
C_{60} bandstructure



- t_{1u} Band ist LUMO
- t_{1u} Band ist dreifach entartet, kann 6 Elektronen aufnehmen
- h_u Band ist HOMO, vollständig gefüllt

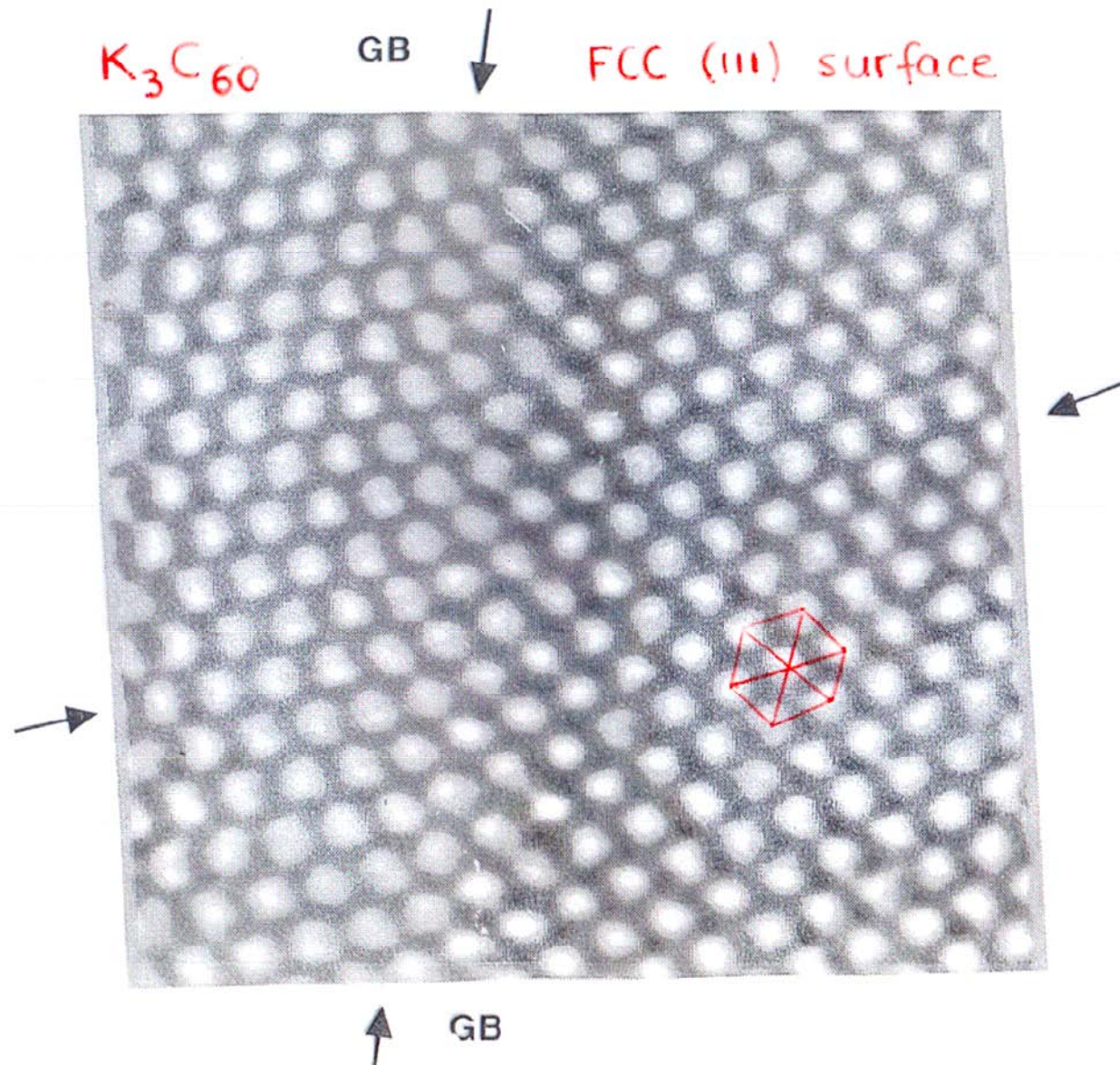


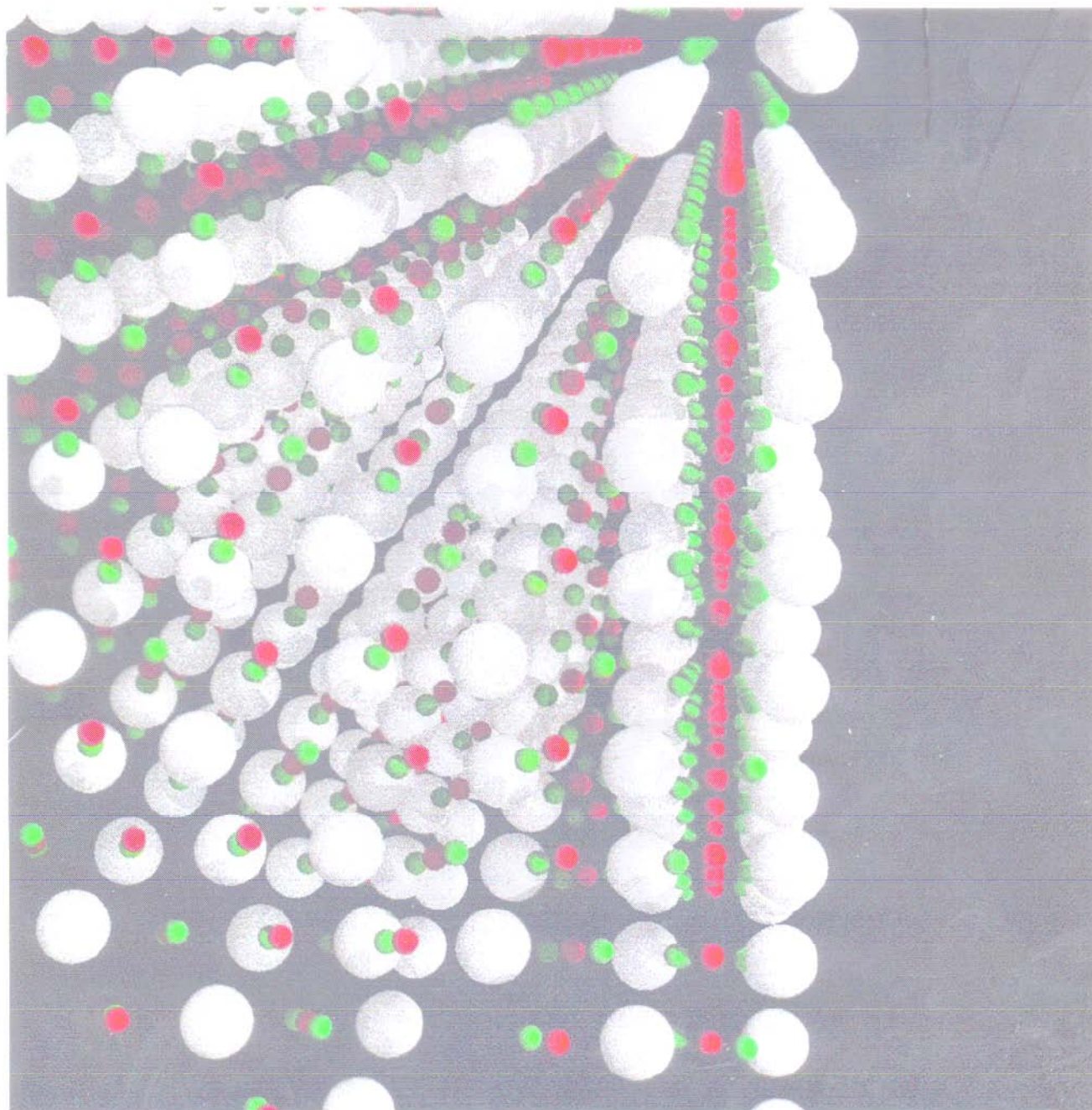
Photoemission : probes only surface layer !

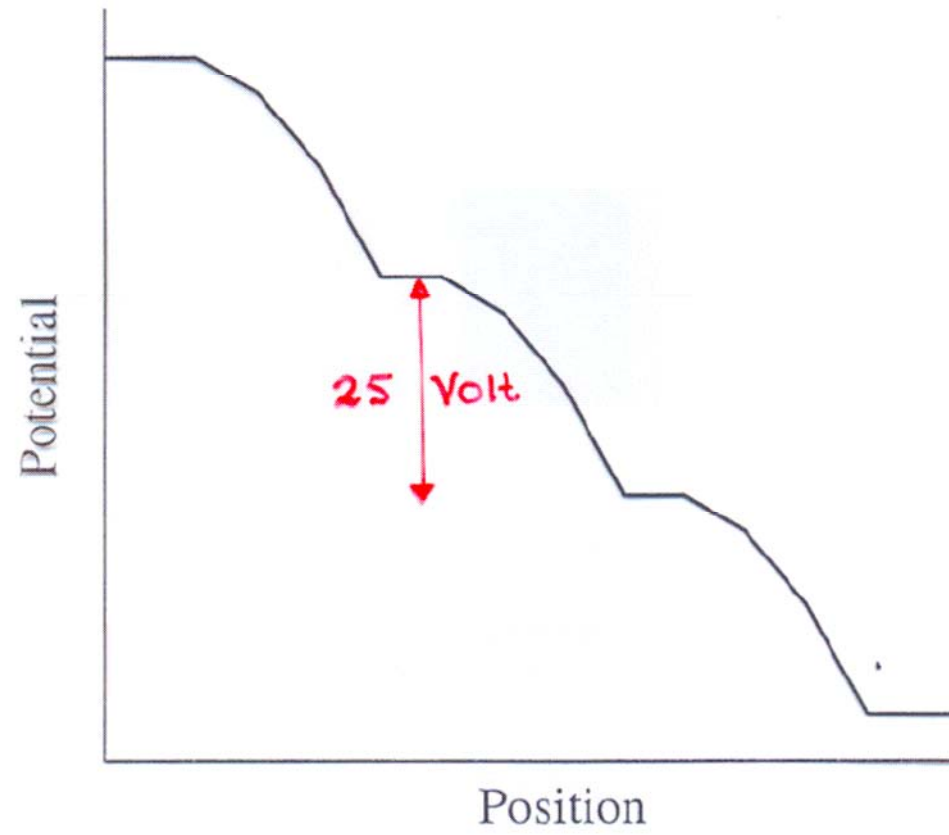
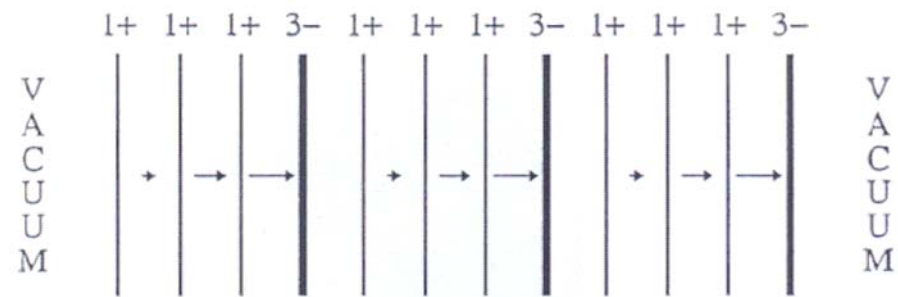


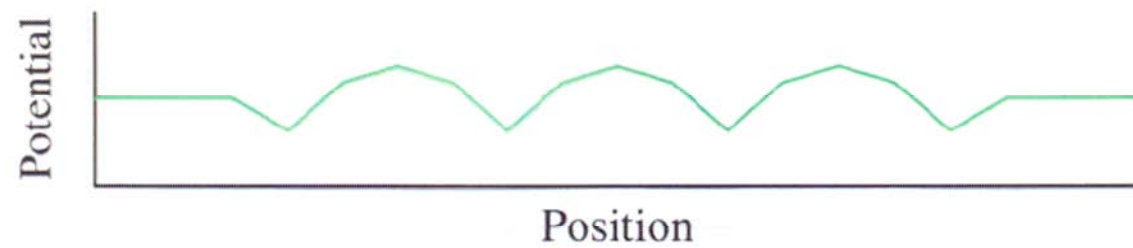
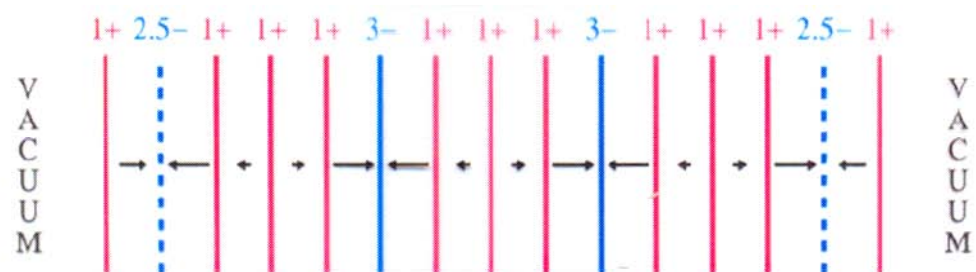
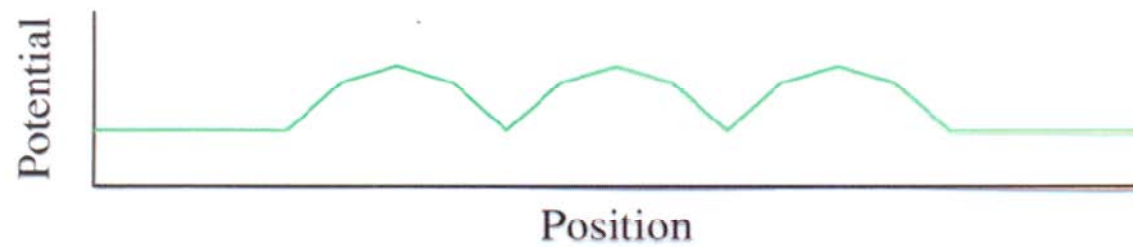
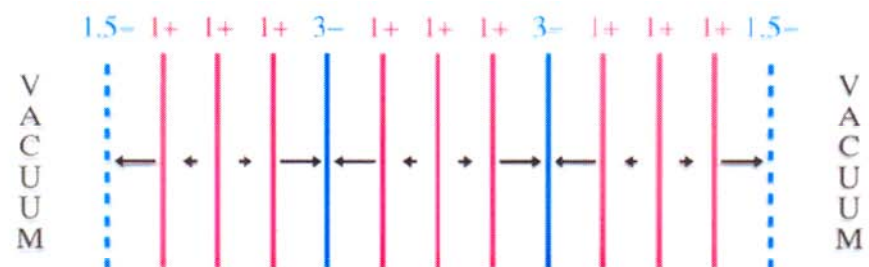
* valence of C_{60} at surface is 2.5^- and not 3^- as in bulk!

J.H. WEAVER AND D.M. POIRIER



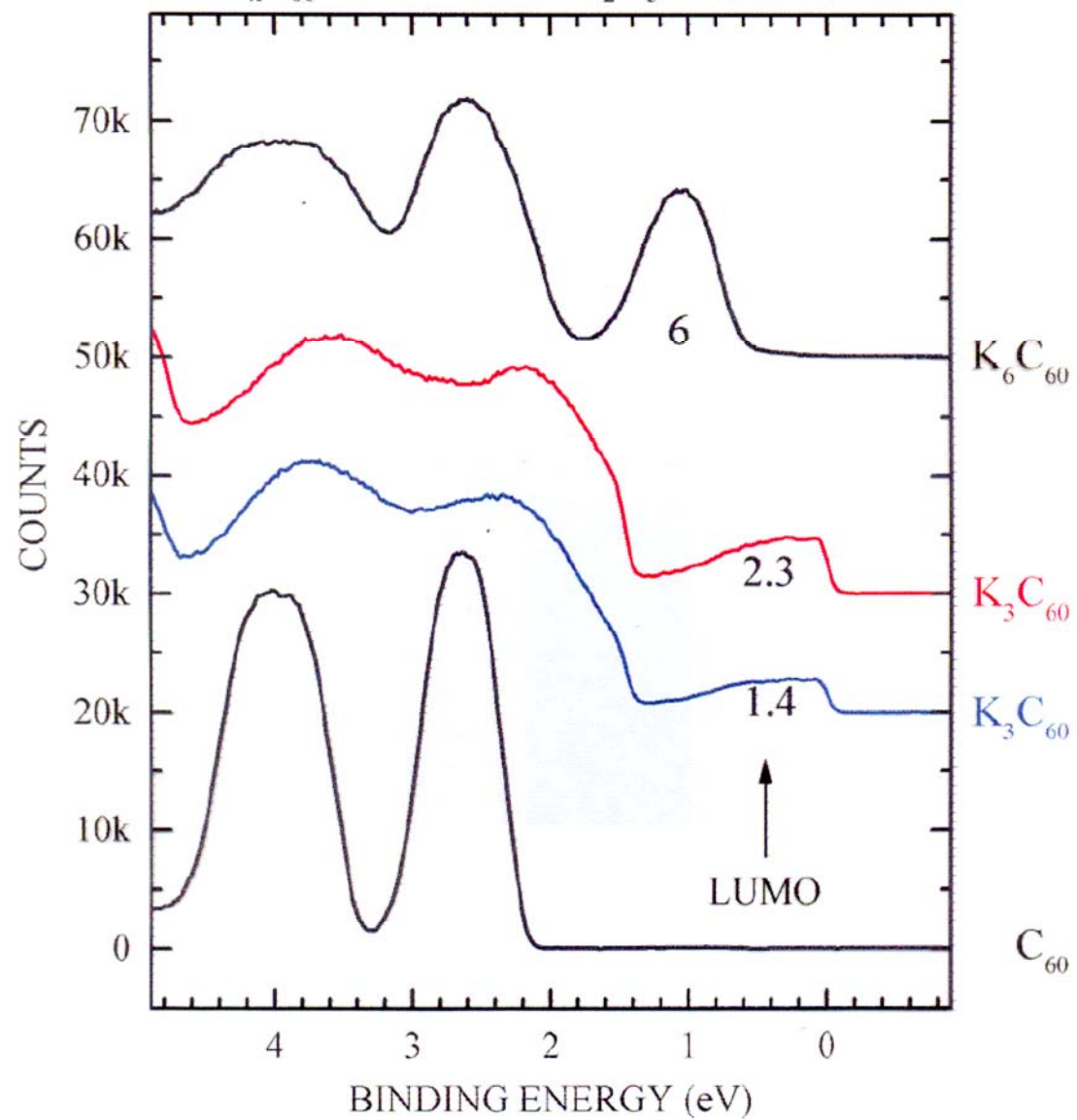






PHOTOEMISSION: $h\nu = 21.2$ eV

$K_x C_{60}$: thin film on Al_2O_3 single crystal



Electronic Structure of K_3C_{60} fcc (111) surface

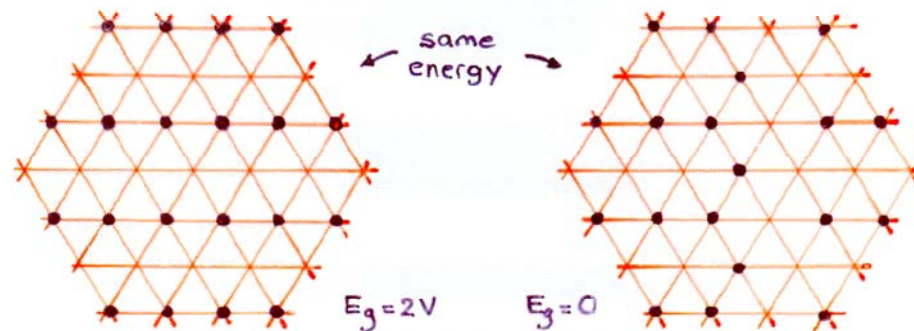
- surface has larger U and smaller W than bulk !
 → naive expectation: bulk is just metallic → surface is insulating

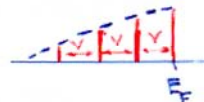
* Integer valence → $\frac{1}{2}$ band filling non-degenerate Hubbard model
 Metal - insulator : $U \gtrless W$

* Integer + $\frac{1}{2}$ valence → $\frac{1}{4}$ band filling non-degenerate Hubbard model
 Metal - insulator : $V \gtrless W$ ($U \gg V$)

U : on-site Coulomb interaction ≈ 1.7 eV
 V : nearest neighbor Coulomb interaction $\approx 0.3 \sim 0.5$ eV
 W : one-electron bandwidth $\approx 0.3 \sim 0.5$ eV

* Triangular lattice, $\frac{1}{4}$ band filling \Rightarrow Frustrated !



Photoemission :  ??

Photoemission from Buried Interfaces in SrTiO₃/LaTiO₃ Superlattices

M. Takizawa,¹ H. Wadati,¹ K. Tanaka,¹ M. Hashimoto,¹ T. Yoshida,¹ A. Fujimori,¹ A. Chikamatsu,² H. Kumigashira,² M. Oshima,² K. Shibuya,³ T. Mihara,⁴ T. Ohnishi,³ M. Lippmaa,³ M. Kawasaki,⁵ H. Koinuma,⁴ S. Okamoto,⁶ and A.J. Millis⁶

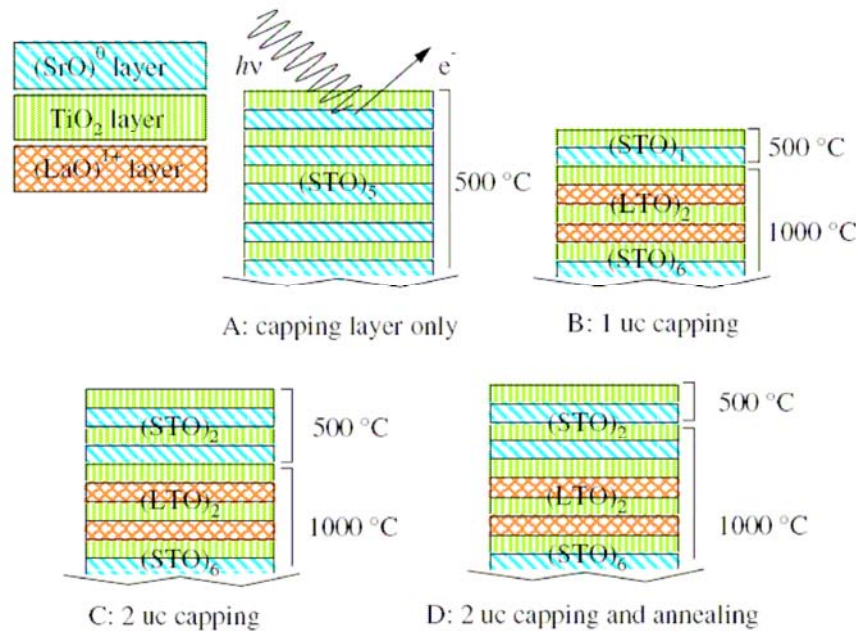


FIG. 1 (color online). Schematic views of the SrTiO₃/LaTiO₃ superlattice samples: capping layer only sample A; 1 uc capping sample B; 2 uc capping sample C; 2 uc capping and annealing sample D. Growth temperatures are also indicated.

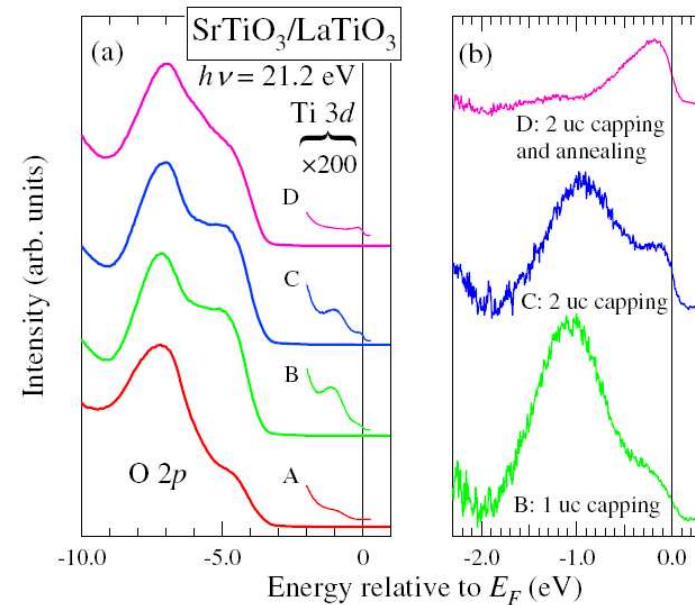
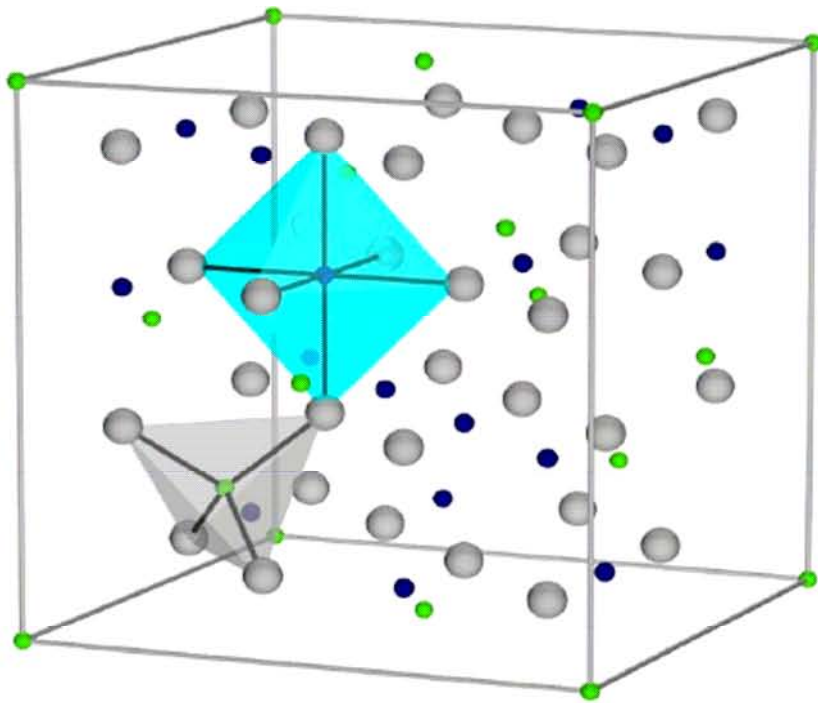


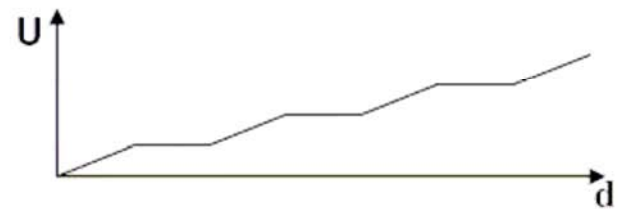
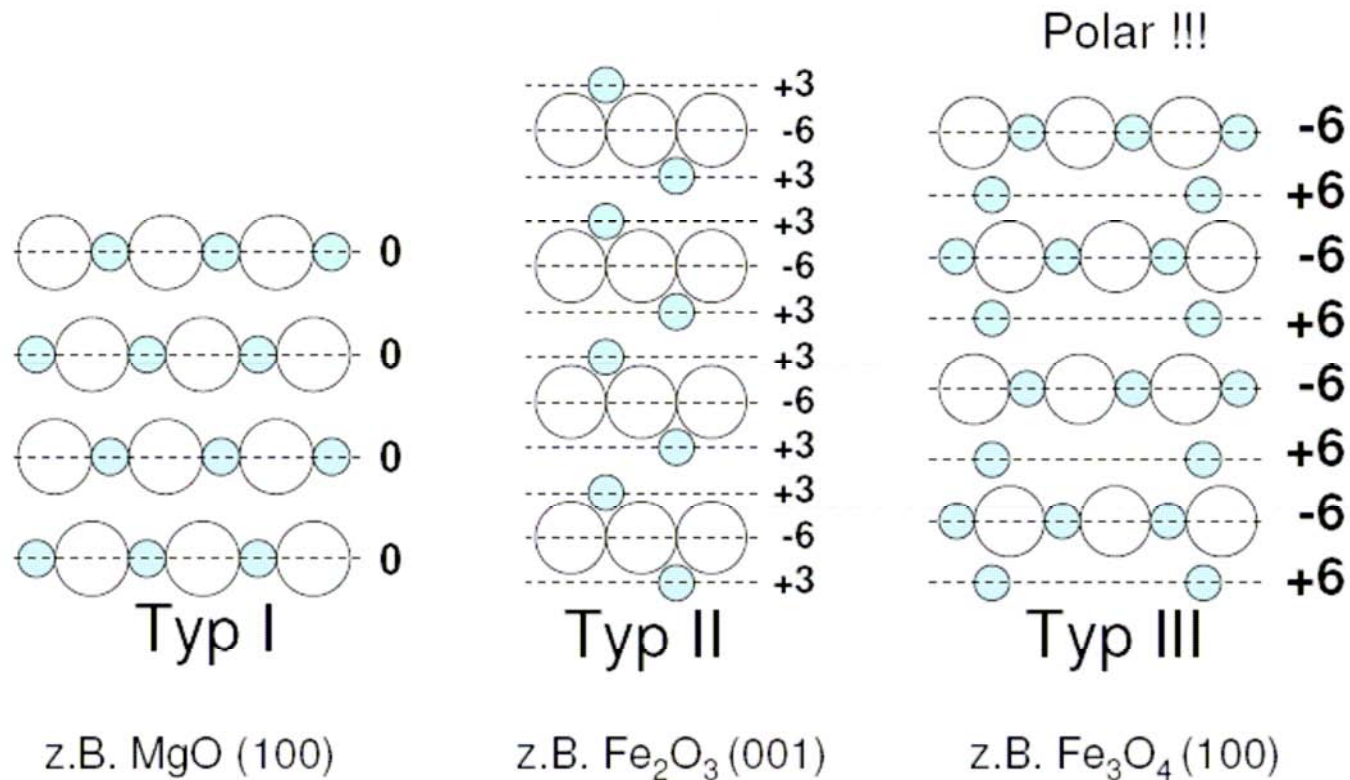
FIG. 2 (color online). UPS spectra of the SrTiO₃/LaTiO₃ superlattice samples: the capping layer only sample A, the 1 uc capping sample B, the 2 uc capping sample C, and the 2 uc capping and annealing sample D. (a) Valence-band spectra over a wide energy range. (b) Near Fermi-level spectra after background subtraction (see text).

Fe_3O_4 : Magnetite



- Ältestes bekanntes magnetische Material
- Natürlich gewachsener Kristall zeigt Oktaederflächen
- Inverse Spinell-Struktur
- Sauerstoff bildet kubisch dichteste Packung
- Eisen füllt Löcher:
 - Trivalente Eisenionen (Fe^{3+}) sind gleichmäßig auf Oktaeder- & Tetraeder-Plätze verteilt
 - Divalente Eisenionen (Fe^{2+}) sind oktaedrisch von O umgeben
- $a = 8.394 \text{ \AA}$

Polar Surface of Fe_3O_4 (100)



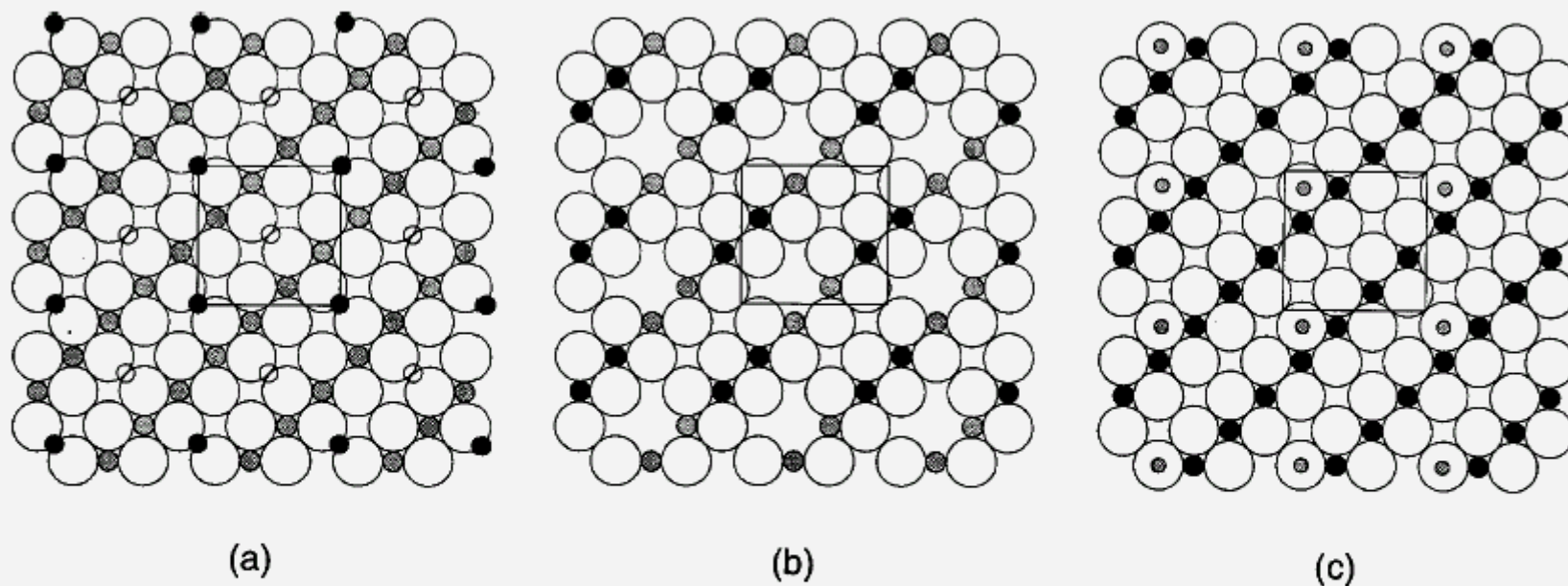
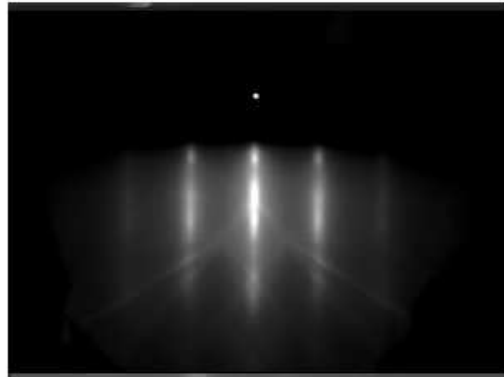


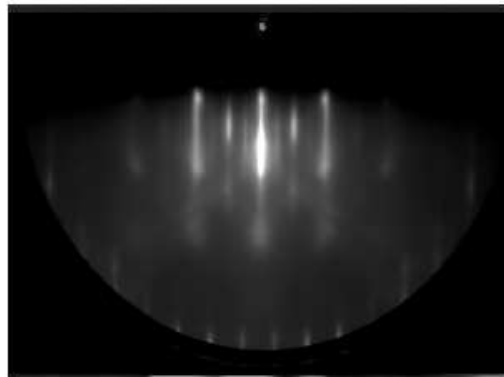
FIG. 7. Three possible surface structures for the $(\sqrt{2} \times \sqrt{2})R45^\circ$ reconstructed $\text{Fe}_3\text{O}_4(100)$ surface, in top view. (a) A termination at a half-filled *A* layer of Fe^{3+} ions. (b) A termination at a *B* layer of oxygen anions and octahedral $\text{Fe}^{2.5+}$ ions. There is one oxygen vacancy per unit cell, accompanied by the oxidation of two $\text{Fe}^{2.5+}$ ions to Fe^{3+} . The remaining $\text{Fe}^{2.5+}$ ions are trapped by the oxygen vacancies, resulting in charge ordering. (c) An alternative termination at a *B* layer. Here, the surface does not contain oxygen vacancies, but one hydroxyl group per unit cell. Furthermore, the surface is fully oxidized, containing only Fe^{3+} ions. Large open circles: oxygen anions; small open circles: missing Fe^{3+} ions; black filled circles: Fe^{3+} ions; large gray filled circles: $\text{Fe}^{2.5+}$ ions; small gray filled circles: hydrogen. In each case, the bulk unit cell is outlined.

RHEED & LEED

RHEED



MgO



Fe₃O₄

LEED



Work in progress

Thin films:

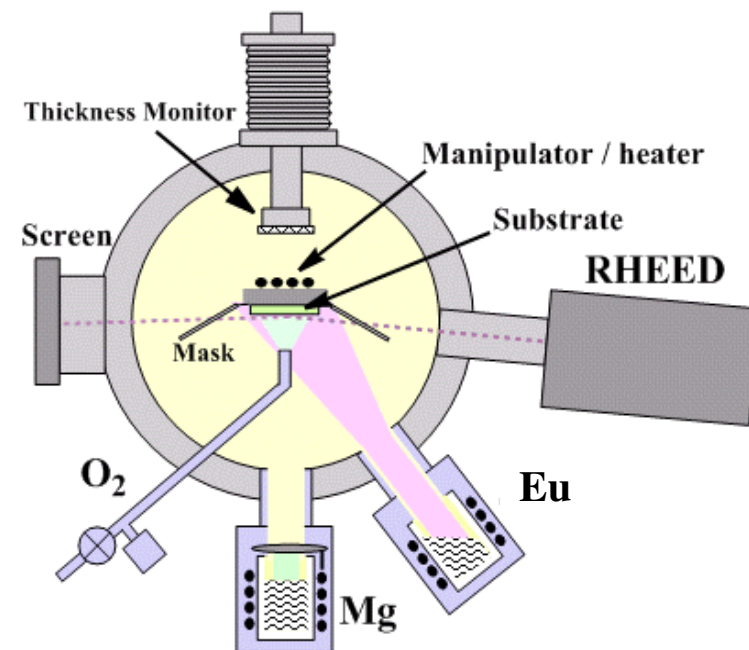
Lehrstuhl für Angewandte Physik, II. Physikalisches Institut

Materials: binary oxides with precise stoichiometry control

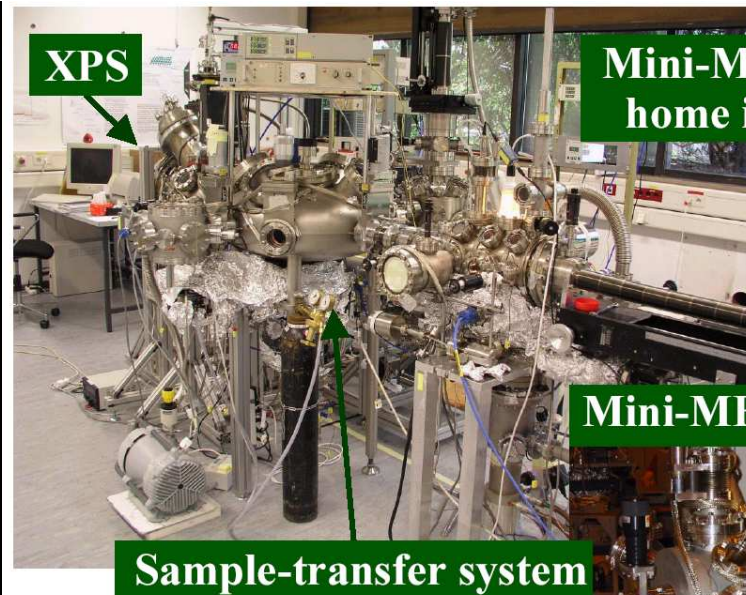
Technique: Molecular Beam Epitaxy

- control of oxygen stoichiometry
- compatible with electron spectroscopies

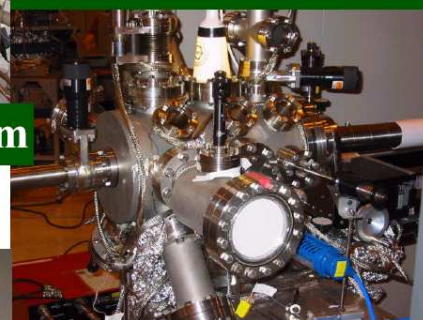
- ultra high vacuum (1×10^{-10} mbar)
- effusion cells and e-beam evaporators
- oxidizers: O_2 , O_3 , NO_2 , O-radicals
- co-evaporation and distillation
- resistivity monitoring during growth !
- in-situ RHEED and LEED
- in-situ XPS and XAS



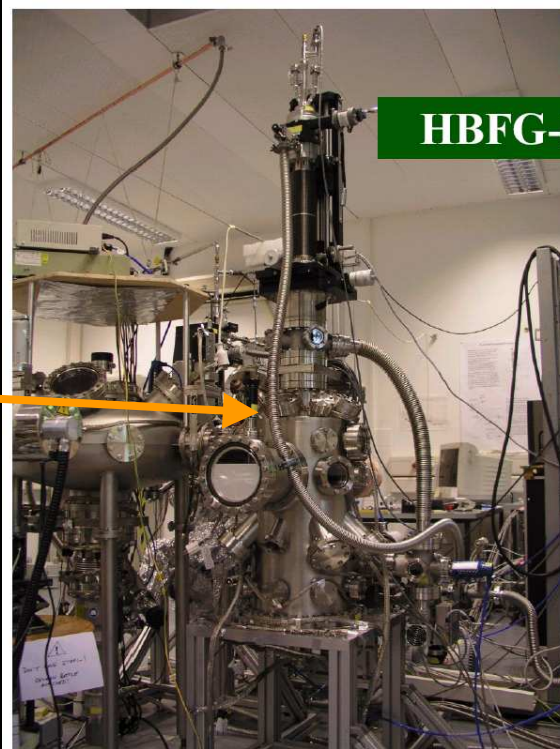
MBE +
in-situ $\rho(T)$



Mini-MBE in Taiwan



identical copies



HBFG-MBE: We have designed and constructed a new more versatile MBE system for the growth of binary oxide systems. It adds to the mini-MBE systems the capability to measure the resistivity of the thin films *in situ* and during growth for a wide range of temperatures. This allows to control the growth condition very accurately and to characterize the temperature-dependent transport properties of the thin films.

The system is equipped with a He flow cryostat, a RHEED gun and screen, and the system can accommodate up to 6 different effusion cells or e-beam evaporators. The design allows a full 360° azimuthal rotation of the sample in order to cover the angular range needed for a complete RHEED analysis.

For maximal flexibility both MBE systems are coupled via a sample-transfer system to each other, to an XPS system and to a loadlock.

Can we use thin films to create new materials, new properties and new devices ?

Yes, but one needs to understand the 'physics', i.e. need to understand what happens to the electronic structure !

- Modification of material properties due to proximity of substrate:
 - strain
 - screening
 - charge donation
- New material compositions:
non-existent in bulk, but stabilized in film
- New sample preparation routes:
MBE combined with distillation and
control of stoichiometry during growth by resistivity measurements